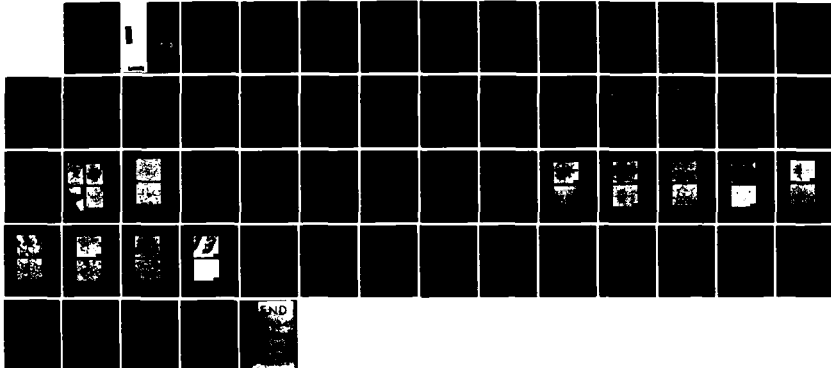
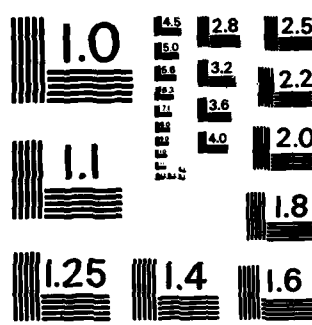


AD-A148 123 MECHANICAL PROPERTIES OF ADHESIVELY BONDED ALUMINUM 1/1  
STRUCTURES PROTECTED W. (U) MARTIN MARIETTA LABS  
BALTIMORE MD G D DAVIS ET AL NOV 84 MML-TR-84-54(C)  
UNCLASSIFIED N00014-80-C-0718 F/G 11/1 NL





MICROCOPY RESOLUTION TEST CHART  
NATIONAL BUREAU OF STANDARDS-1963-A

MARTIN MARIETTA

Martin Marietta  
Laboratories

12

MML-TR-84-54(c) ✓

MECHANICAL PROPERTIES OF ADHESIVELY  
BONDED ALUMINUM STRUCTURES PROTECTED  
WITH HYDRATION INHIBITORS

End-of-Fourth Year Report on  
ONR Contract N00014-80-C-0718

November 1984

DTIC  
SELECTED  
NOV 26 1984  
S D  
B

Prepared for:

Department of the Navy  
Office of Naval Research  
Arlington, Virginia 22217

Prepared by:

MARTIN MARIETTA CORPORATION  
Martin Marietta Laboratories  
1450 South Rolling Road  
Baltimore, Maryland 21227

NON STATEMENT A  
for public release  
by unlimited

84 11 14 222

REPORT DOCUMENTATION PAGE		READ INSTRUCTIONS BEFORE COMPLETING FORM
1. REPORT NUMBER	2. GOVT ACCESSION NO.	3. RECIPIENT'S CATALOG NUMBER
AD-A14 8123		
4. TITLE (and Subtitle) Mechanical Properties of Adhesively Bonded Aluminum Structures Protected with Hydration Inhibitors	5. TYPE OF REPORT & PERIOD COVERED End-of-Fourth-Year Report	
7. AUTHOR(s) G.D. Davis, J.S. Ahearn, L.J. Matienzo, and J.D. Venables	6. PERFORMING ORG. REPORT NUMBER MML TR 84-54(c)	
9. PERFORMING ORGANIZATION NAME AND ADDRESS Martin Marietta Laboratories 1450 South Rolling Road Baltimore, Maryland 21227	8. CONTRACT OR GRANT NUMBER(s) N00014-80-C-0718	
11. CONTROLLING OFFICE NAME AND ADDRESS Department of the Navy Office of Naval Research Arlington, Virginia 22217	12. REPORT DATE November 1984	
14. MONITORING AGENCY NAME & ADDRESS (if different from Controlling Office) Baltimore DCAS Management Area 300 East Joppa Road, Room 200 Towson, Maryland 21204	13. NUMBER OF PAGES 49	
16. DISTRIBUTION STATEMENT (of this Report) Unlimited distribution	15. SECURITY CLASS. (of this report) 15a. DECLASSIFICATION/DOWNGRADING SCHEDULE	
DISTRIBUTION STATEMENT A Approved for public release Distribution Unlimited		
17. DISTRIBUTION ST. AGENT (of this abstract entered in Block 20, if different from Report)		
18. SUPPLEMENTARY FES		
19. KEY WORDS (Continue on reverse side if necessary and identify by block number) Adhesive bonding, organic inhibitors, mechanical testing, aluminum.		
20. ABSTRACT (Continue on reverse side if necessary and identify by block number) The use of several amino phosphonic acids as hydration inhibitors to improve the properties of adhesively bonded aluminum structures has been investigated using T-peel, double-lap-shear, and wedge tests. Each of the inhibitors tested was found to be compatible with epoxy adhesives in a dry environment. Most were also compatible in a hot, humid environment. Examination of both sides of the propagated crack in wedge test specimens treated with nitrilotris methylene phosphonic acid (NTMP) showed that hydration of the oxide could be slowed		

sufficiently so that crack propagation occurred prior to it. In this case, the weakest link was the coupling of the inhibitor to the adhesive. Inhibitors designed to strengthen this coupling have been synthesized and are currently being tested.

ii

Accession For	
NTIS	GRA&I
DTIC TAB	<input checked="" type="checkbox"/>
Unannounced	<input type="checkbox"/>
Justification	<input type="checkbox"/>
By _____	
Distribution/	
Availability Codes	
Dist	Avail and/or Special
A-1	

MML TR 84 - 54C

*ADHESIVELY*  
MECHANICAL PROPERTIES OF ALUMINUM BONDED  
ALUMINUM STRUCTURES PROTECTED WITH HYDRATION INHIBITORS

End-of-Fourth-Year Report on  
ONR Contract N00014-80-C-0718

November, 1984

Prepared for:

Department of the Navy  
Office of Naval Research  
Arlington, Virginia 22217

Prepared by:

G.D. Davis, J.S. Ahearn, L.J. Matienzo, and J.D. Venables  
Martin Marietta Laboratories  
1450 South Rolling Road  
Baltimore, Maryland 21227

  
G.D. Davis  
Principal Investigator

TABLE OF CONTENTS

	<u>PAGE</u>
LIST OF FIGURES	iii
LIST OF TABLES	v
ABSTRACT	vi
I. INTRODUCTION	1
II. EXPERIMENTAL	3
A. MECHANICAL TESTING	3
B. ANALYSIS	4
C. INHIBITORS	6
III. RESULTS	9
A. INITIAL DRY STRENGTH	9
B. BOND DURABILITY	14
IV. DISCUSSION	23
A. INITIAL DRY STRENGTH	23
B. BOND DURABILITY	23
V. SUMMARY	26
VI. REFERENCES	27
APPENDICES	
A. OXIDE MORPHOLOGIES	37
B. SYNTHESIS	42

## LIST OF FIGURES

- Figure 1. Inhibitors tested in this program: a) denotes compounds commercially available, and b) denotes compounds synthesized here.
- Figure 2. Additional inhibitors synthesized and tested based on criteria discussed in Section IV.
- Figure 3. Wedge-test results (crack length as a function of time) for FPL adherends treated in solution of MP, AMP, (nBu)NBMP, and NTMP and for untreated FPL adherends.<sup>(11)</sup>
- Figure 4. Wedge-test results (crack length as a function of time) for FPL adherends treated in solutions of AMP, (nBu)NBMP, NTMP, and EDTMP.
- Figure 5. Wedge-test results (crack length as a function of time) for FPL adherends treated in solutions of PA.<sup>(9)</sup>
- Figure 6. Scanning electron micrographs of the near-crack-tip region of the aluminum side of an NTMP-treated FPL-etched wedge test specimen: a) low magnification view showing 1) the dull aluminum area and 2) the shiny aluminum area, and the cohesive failure in the adhesive after the wedge test was completed (at right); b) the beginning of hydration in the boundary region between dull and shiny areas, enlargement of the blocked-in area in inset is at left; c) higher magnification stereo view of the dull area showing the corn-flake boehmite structure; and d) high-magnification stereo view of the shiny area showing the original FPL morphology.
- Figure 7. Scanning electron micrographs of the near-crack-tip region of the aluminum side of two inhibitor-treated FPL-etched wedge test specimens: a) AMP-treated surface exhibiting cornflake (boehmite) morphology and b) (nBu)NBMP-treated surfaces exhibiting bayerite crystallites on top of boehmite.
- Figure 8. Wedge-test results (crack length as a function of time) for FPL adherends treated in solutions of 2pA, NTMP, 2 , EDTMP, (nBu)NBMP, and (nBu)ANBMP and for untreated FPL adherends.

LIST OF FIGURES (Continued)

- Figure A1. XSEM micrographs of the FPL-etched 2024 Al surface.
- Figure A2. XSEM micrographs of the FPL-etched 6061 Al surface.
- Figure A3. XSEM micrographs of the FPL-etched 7005 Al surface.
- Figure A4. XSEM micrographs of the PAA-treated 2024 Al surface.
- Figure A5. XSEM micrographs of the PAA-treated 6061 Al surface.
- Figure A6. XSEM micrographs of the PAA-treated 7005 Al surface.
- Figure A7. XSEM micrographs of the P2-etched 2024 Al surface.
- Figure A8. XSEM micrographs of the P2-etched 6061 Al surface.
- Figure A9. XSEM micrographs of the P2-etched 7005 Al surface.

## LIST OF TABLES

	<u>PAGE</u>
Table 1. Mechanical Testing Parameters	5
Table 2. T-peel Strengths	10
Table 3. Surface Compositions (at. %) of Adjoining T-peel Sides	11
Table 4. Double Lap Shear Strengths	12
Table 5. Surface Composition of Wedge Test Surfaces (at. %)	17
Table A1 Aluminum Pretreatments for Adhesive Bonding	38
Table A11 Pretreatment Solutions	39

ABSTRACT

The use of several amino phosphonic acids as hydration inhibitors to improve the properties of adhesively bonded aluminum structures has been investigated using T-peel, double-lap-shear, and wedge tests. Each of the inhibitors tested was found to be compatible with epoxy adhesives in a dry environment. Most were also compatible in a hot, humid environment. Examination of both sides of the propagated crack in wedge test specimens treated with nitrilotris methylene phosphonic acid (NTMP) showed that hydration of the oxide could be slowed sufficiently so that crack propagation occurred prior to it. In this case, the weakest link was the coupling of the inhibitor to the adhesive. Inhibitors designed to strengthen this coupling have been synthesized and are currently being tested.

## I. INTRODUCTION

The quality of an adhesive bond is determined by its initial strength and its strength over time. The microscopically rough aluminum oxide formed by commercial aerospace bonding processes<sup>(1,2)</sup> provides opportunities for mechanical interlocking between the oxide and polymeric adhesive<sup>(3,4)</sup> and results in high bond strength for structures exposed only to dry environments. In fact, crack propagation in properly prepared structures using most adhesives occurs within the adhesive indicating that the strength of the polymer controls the strength of the structure.

In hot, humid environments, however, the strength of bonded structures, especially those prepared by the Forest Product Laboratory (FPL)<sup>(1)</sup> process, is dramatically degraded. In these cases, crack propagation is facilitated by hydration of the aluminum oxide to the oxyhydroxide, boehmite. This transformation causes dramatic volume and morphology changes which, in turn, induce large stresses at the bond line and resultant failure at the boehmite-metal or boehmite-adhesive interfaces.<sup>(5-8)</sup>

Such findings have prompted us to investigate methods to inhibit the oxide-to-hydroxide conversion process with the goal of improving the long-term durability of adhesively bonded aluminum structures. One such procedure is to treat an FPL adherend with certain organic acids (amino phosphonates). These surfaces, with a saturation inhibitor coverage of approximately one monolayer, exhibit a much higher resistance to hydration (up to two orders of magnitude) than untreated FPL surfaces and have a corresponding increase in the long-term bond durability.<sup>(8-9)</sup>

In the previous years of this program (ONR N00014-80-C-0718),<sup>(6,10,11)</sup> we examined the adhesive bond mechanical properties and surface chemistry of FPL and phosphoric-acid-anodized (PAA) adherends treated with hydration inhibitors, particularly nitrilotris methylene phosphonic acid (NTMP,  $\text{N}[\text{CH}_2\text{PO}(\text{OH})_2]_3$ ) and related compounds. We showed that: 1) NTMP-treated FPL

bonds and PAA bonds exhibited similar long-term durability, 2) the durability of NTMP-treated PAA bonds was better than untreated PAA bonds, 3) adsorption of these inhibitors involved the displacement of water initially present on the aluminum oxide surface and the formation of P-O-Al bonds, 4) hydration of treated surfaces was limited by the dissolution of the monolayer inhibitor-Al complex, and 5) an inhibitor's effectiveness depended both on its ability to inhibit the oxide-to-hydroxide conversion and on its compatibility with the adhesive.

Based on these findings, we identified four criteria of an inhibitor to promote good bond performance: 1) occupation of all active sites on the Al<sub>2</sub>O<sub>3</sub> surface, 2) strong inhibitor-surface bonds, 3) insolubility of the resulting inhibitor-aluminum complex in aqueous solutions, and 4) compatibility with the adhesive/primer.

In the continuation of this program we have designed, synthesized, and tested several new variants of the NTMP molecule in attempts to: 1) determine any additional criteria which may be important in achieving bond durability, and 2) enhance the inhibitor's effectiveness in improving bond performance.

To this end, we have tested both treated and untreated structures using: 1) T-peel and double-lap-shear tests to examine any effect of the inhibitor on the initial bond strength and 2) wedge tests to establish the effectiveness of the inhibitor in increasing bond durability. At the conclusion of these tests, the failure surfaces were examined by x-ray photoelectron spectroscopy (XPS) and high resolution scanning electron microscopy (XSEM) in order to determine the locus of crack propagation.

As a supplementary project, we have examined the oxide morphologies of 6061 and 7005 Al alloys, commonly used in mobile bridge construction, and compared them with the corresponding morphologies of 2024 Al, the alloy otherwise used in this program. These results are presented as Appendix I.

## II. EXPERIMENTAL

### A. MECHANICAL TESTING

Bare test panels of 2024, 6061, and 7005 Al were degreased by 15-minute immersion in an agitated solution of Turco 4215\* (44 g/l) at 65°C and then rinsed in distilled, deionized water. Degreasing was followed by a standard FPL treatment, consisting of a 15-minute immersion in an agitated aqueous solution of sodium dichromate dihydrate (60 g/l) and sulfuric acid (17% v/v) held at 65°C, after which samples were rinsed in distilled, deionized water and air dried.

Some 2024 Al panels were immersed for 15-30 minutes in a dilute aqueous solution of an inhibitor held at room temperature or, in special cases, at 80°C. Solution concentrations ranged from 10 to 100 ppm for the T-peel experiments and from 100 to 300 ppm for the wedge and double-lap-shear tests. The samples were then thoroughly rinsed in distilled deionized water and forced-air dried.

Panels for wedge tests (6 x 6 x 0.125 in.) were bonded together using American Cyanamid FM 123-2 adhesive cured at 120°C and 40 psi for 1 hour. The bonded panels were cut into 1 x 6 in. test strips and a wedge (0.125-in. thick) was inserted between the two adherends to provide a stress at the bondline (ASTM D-3762). After 1-hour equilibration at ambient conditions, the wedge-test samples were placed in a humidity chamber held at 60°C and 98% relative humidity. In order to determine the extent of crack propagation, we periodically removed the test pieces from the humidity chamber and examined them under an optical microscope, locating and marking the position of the

---

\*An alkaline cleaning agent manufactured by Turco Products.

crack front. When the test was complete, usually after 150 to 160 hours, calipers were used to measure the positions of these marks, which denote crack length as a function of time.

Other panels for T-peel tests ( $6 \times 12 \times 0.032$  in.) were bonded together using the adhesives and cures listed in Table I. The panels were then cut into 1-in. strips and pulled using an Instron Model 1128 Tensile Testing machine with a cross head speed of 200 mm/min.

Double lap shear specimens, with a bond area of  $1 \times 0.5$  in. on each side of the center panel (modified ASTM D 3528 Type A), were constructed using either FM 123-2 or Cybond 1102 as described in Table I. Adhesive thickness for the Cybond 1102 was controlled by a loop of 8-mil wire. The structures were then pulled using an Instron Model TTCL tensile testing machine with a cross-head speed of 0.13 mm/min.

## B. ANALYSIS

The surface chemistry and morphology of the failed surfaces of the wedge and T-peel tested specimens were frequently examined by XPS or XSEM, respectively. The XPS measurements were made on a Physical Electronics Model 548 spectrometer, which consists of a double-pass cylindrical mirror analyzer (CMA) with pre-retarding grids and a coaxial electron gun, a Mg anode X-ray source, a rasterable 5-keV sputter ion gun, a sample introduction device, and a gas-handling system used to backfill the chamber to  $5 \times 10^{-5}$  Torr Ar. A PDP 1104 minicomputer was used to control data acquisition and analysis. Operating pressure typically was in the low  $10^{-9}$  Torr range. Atomic concentrations were determined from survey spectra using sensitivity factors for the O1s, Al2p, and P2p peaks measured from standards on this instrument. (12)

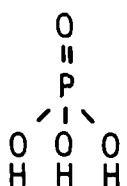
Table I  
Mechanical Testing Parameters

<u>Adhesive</u>	<u>Chemistry</u>	<u>Cure</u>	<u>Test</u>
FM 123-2	Nitrile Epoxy	120°C, 40 psi-1 hr	Wedge, Double-Lap-Shear
FM 123-5	Nitrile Epoxy	110°C, 40 psi-45 min	T-peel
FM 238/BR 238	Nitrile Phenolic	170°C, 40 psi-1 hr	T-peel
FM 1000-EP15	Polyamide Epoxy	170°C, 40 psi-1 hr	T-peel
FM 53	Epoxy	120°C, 40 psi-1 hr	T-peel
Cybond 1102	Polyamide Epoxy	RT, 7.5 psi-7 days	Double-Lap-Shear

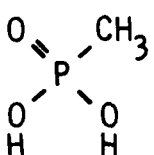
The XSEM micrographs, which were also used to compare the oxide morphologies of the three aluminum alloys (Appendix A), were obtained with a JEOL-100CX scanning transmission electron microscope (STEM) operated in the high resolution (30 Å) SEM mode. Charging of the surface by the electron beam was suppressed by depositing an extremely thin Pt coating on the surface of the specimens using secondary ion deposition.

C. INHIBITORS

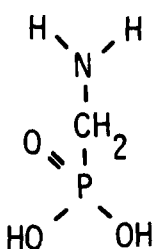
The inhibitors shown in Figs. 1 and 2 were selected or designed to test different aspects of an inhibitor system, including bonding to the Al<sub>2</sub>O<sub>3</sub> surfaces and coupling, chemically or physically, with the adhesive. Some of the inhibitors are commercially available; others were synthesized (some for the first time) prior to testing. The details of the syntheses are described in Appendix B.



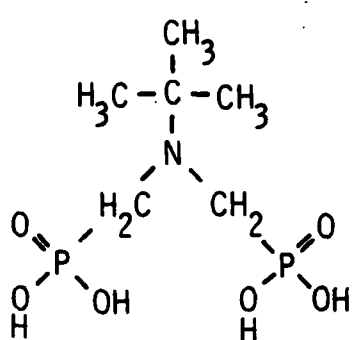
Phosphoric Acid<sup>a</sup>  
[PA]



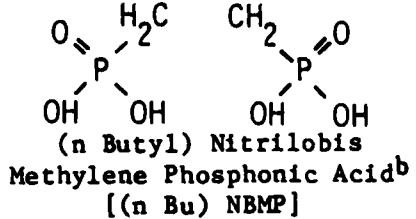
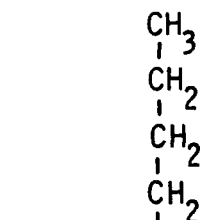
Methylene  
Phosphonic Acid<sup>a</sup>  
[MP]



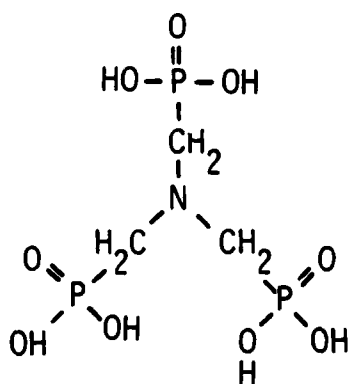
Amino Methylenephosphonic Acid<sup>a</sup>  
[AMP]



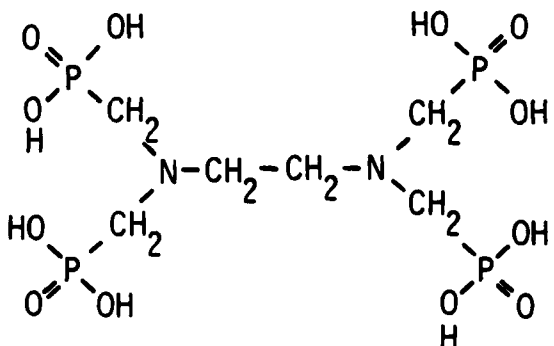
(t Butyl) Nitrilobis  
Methylene Phosphonic Acid<sup>b</sup>  
[(t Bu) NBMP]



(n Butyl) Nitrilobis  
Methylene Phosphonic Acid<sup>b</sup>  
[(n Bu) NBMP]



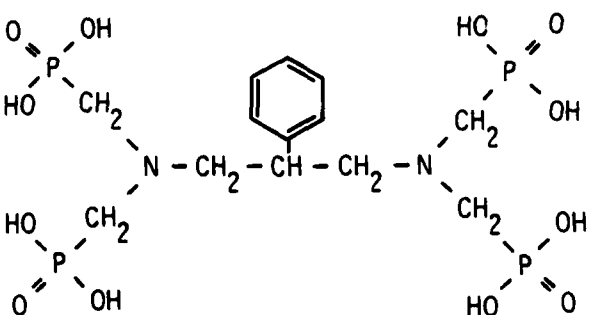
Nitrilotris Methylene  
Phosphonic Acid<sup>a</sup> [NTMP]



Ethylene Diamine Tetramethylene  
Phosphonic Acid<sup>b</sup> [EDTMP]

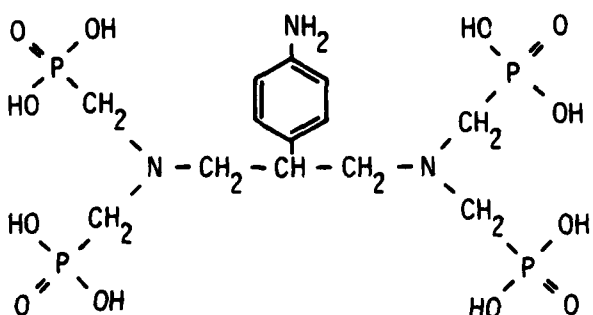
Figure 1. Inhibitors tested in this program: a) denotes compounds commercially available, and b) denotes compounds synthesized here.

2Φ



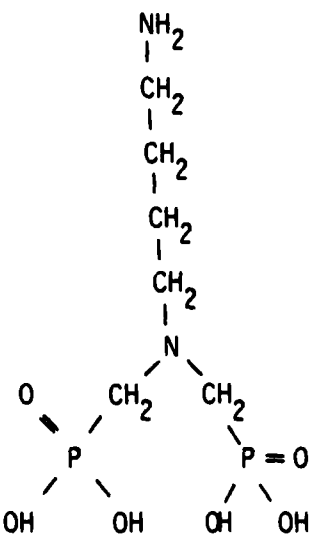
2-phenyl 1,3-di (nitrilobismethylene phosphonic acid) propane

2pA



2-p-anilino 1,3-di (nitrilobismethylene phosphonic acid) propane

(nBu)ANBMP



## (n-butyl) aminonitrilobis methylene phosphonic acid

**Figure 2.** Additional inhibitors synthesized and tested based on criteria discussed in Section IV.

### III. RESULTS

#### A. INITIAL DRY STRENGTH

Mechanical testing of inhibitor-treated adherends has concentrated in two areas: dry strength and durability in a humid environment. The dry strength of treated structures was compared to that of control structures using a variety of adhesives in T-peel and double lap-shear tests to determine the compatibility of different adhesive-inhibitor systems. The T-peel strength values are given in Table II. For most adhesives, three classes of inhibitors were tested: NTMP, which is our standard compound; (nBu)NBMP, which has an exposed inert hydrocarbon chain; and MP, which is the simplest phosphonic acid. For each of the epoxy adhesives tested, the treated structures, including those with supermonolayer coverages of inhibitors<sup>(9)</sup>, exhibited the same pull strengths as the control FPL structures, indicating no degradation of the dry interfacial strength. In fact, failure of the specimens examined by XPS occurred cohesively in the adhesive as shown by the high C and low O concentrations on each side (Table III). Such a failure mode represents the best performance of any given adhesive structure and indicates that the "weakest link" of the system is tensile strength of the polymer. The behavior of the samples bonded with a nitrile phenolic is different. For unprimed structures (a procedure not recommended with FM 238), a significant degradation of pull strength occurred upon inhibitor treatment, especially with (nBu)NBMP. For primed structures, only a slight degradation was measured. Failure in both cases occurred with polymeric material, suggesting that the inhibitor may have weakened the unprimed adhesive, perhaps by interfering with the cure or by modifying its wetting ability.

The double lap shear results, shown in Table IV, gave very similar results for two epoxy adhesives, including one cured at room temperature. No degradation of the dry strength was seen following inhibitor treatment.

Table II  
T-peel Strengths  
Adhesives

Treatment	FM-123-5 Nitrile Epoxy	FM 238a Nitrile Phenolic	FM 238/BR238 <sup>b</sup> Nitrile Phenolic	FM1000 Polyamide Epoxy	FM 53 Epoxy
Control	24.9 ± 3.8 lb/in.	29.2 ± 3.3 lb/in.	37.5 ± 3.1 lb/in.	80.3 ± 1.9 lb/in.	50.9 ± 4.6 lb/in.
NP 300ppm	22.0 ± 2.3	17.4 ± 2.5	20.1 ± 2.6	-----	-----
NMP	-----	-----	-----	-----	-----
10ppm, RT	32.6 ± 3.3	21.1 ± 2.9	28.3 ± 1.6	83.6 ± 1.6	50.7 ± 7.8
100ppm, RT	23.8 ± 0.8	15.6 ± 2.7	23.8 ± 0.9	79.8 ± 0.9	51.2 ± 5.2
100ppm, 80°C	22.6 ± 1.5	7.9 ± 1.8	29.6 ± 1.8	83.6 ± 0.0	-----
(nBu) <sub>4</sub> Nep	-----	-----	-----	-----	-----
10ppm, RT	23.4 ± 0.9	c	34.9 ± 1.6	82.5 ± 1.1	-----
100ppm, RT	24.0 ± 1.8	< 5	26.9 ± 2.6	82.5 ± 1.1	-----
100ppm, 80°C	23.0 ± 2.0	< 5	24.5 ± 1.1	83.6 ± 0.0	-----
Failure-Visual	Cohesive	Adhesive	Adhesive/Adhesive	Cohesive	Cohesive
XPS	-----	-----	-----	-----	-----

a Not primed

b Primed with BR 238

c 2 samples averaged 13.8 lb/in., 4 samples < 5 lb/in.

d Between primer and adhesive

Table III  
Surface Compositions (at. %) of Adjoining T-peel Sides

Adhesive	Inhibitor	M <sup>a</sup>	A1	A2	M <sup>a</sup>	0	A <sup>a</sup>	M <sup>a</sup>	C	M <sup>a</sup>	A <sup>a</sup>	M <sup>a</sup>	Other	A <sup>a</sup>	M <sup>a</sup>	Failure Mode
FM238/BR238	Control	---	---	11.0	8.3	77.6	82.1	N = 4.0	N = 5.2	S1 = 7.3	S1 = 4.4	---	---	---	---	cohesive b
FM238/BR238	NTIP 100ppm	1.7	---	12.2	9.1	79.0	78.7	N = 4.7	N = 5.6	S1 = 2.4	S1 = 6.3	---	---	---	---	cohesive b
FM238/BR238	(nBu)NHP 100ppm	---	---	9.7	11.2	80.9	76.6	S = 0.4	N = 4.7	N = 3.9	S1 = 6.3	---	---	---	---	cohesive b
FM238/BR238	Control	1.1	0.6	16.5	14.3	70.8	75.4	N = 5.7	N = 8.7	S1 = 3.9	S1 = 1.0	---	---	---	---	cohesive
FM1000EP15	NTIP 100ppm	1.2	---	22.3	18.1	66.1	73.9	N = 3.9	N = 7.0	S1 = 6.5	S1 = 1.1	---	---	---	---	cohesive
FM1000EP15	(nBu)NHP 100ppm	2.6	---	20.6	14.4	68.3	75.3	N = 5.4	N = 7.6	S1 = 3.1	S1 = 2.7	---	---	---	---	cohesive
FM238	control	---	---	6.6	4.5	87.0	87.4	N = 6.4	S = 0.4	N = 7.6	N = 7.6	---	---	---	---	cohesive
FM238	NTIP 100ppm	---	---	8.6	4.5	86.8	88.0	N = 4.6	N = 6.0	S1 = 4.6	S1 = 1.5	---	---	---	---	cohesive
FM238	(nBu)NHP 100ppm	4.9	3.1	17.2	10.0	78.0	84.3	----	----	----	----	---	---	---	---	cohesive

a) M = metal side; A = adhesive side

b) cohesive with primer/adhesive system

Table IV  
Double Lap Shear Strengths

<u>Treatment</u>	<u>Adhesives</u>
	FM123-2
Control	3900 lb/in. <sup>2</sup>
NTMP 100 ppm	3900 lb/in. <sup>2</sup>
Failure Visual	cohesive
	Cybond 1102
	2600 lb/in. <sup>2</sup>
	2700 lb/in. <sup>2</sup>
	cohesive/adhesive

## B. BOND DURABILITY

The effectiveness of inhibitors to improve bond durability (the primary goal of these compounds) was determined using wedge tests on treated adherends. The first set of tests, using the inhibitors shown in Figure 1, are presented in Figs. 3-5.

Based on these results, we have classified the inhibitors into three groups: (I) MP and PA, which provide either worse performance or no improvement over the untreated FPL specimens; (II) AMP and (tBu)NBMP, which provide some improvement over the control; and (III) NTMP, (nBu)NBMP, and EDTMP, which provide the best performances. In each case, however, the performance is not as good as that limited by the adhesive<sup>(7)</sup> (Fig. 3).

To determine the locus of failure of the wedge-test specimens, X-SEM micrographs and/or XPS measurements of the near-crack-tip region were obtained for selected samples in each of the three groups. The XPS results are summarized in Table V. The failure of MP-, PA-, NTMP-, and EDTMP-treated specimens occur near or at the adhesive-adherend interface because substantial differences are seen between the metal and adhesive sides of the failure with Al (and O) denoting aluminum oxide or hydroxide and high C denoting the adhesive. (Al and some O on the adhesive side of NTMP- and EDTMP-treated bonds result from aluminum hydroxides which are solution-deposited from the condensed water vapor. Similarly the C on the metal side results from adventitious hydrocarbon contamination.) In contrast, the two surfaces of the FPL control and specimens treated with (tBu)NBMP and (nBu)NBMP exhibit high Al and O and low C indicating that the locus of failure is in the oxide/hydroxide or at the interface between the oxide/hydroxide and the metal with subsequent hydration or corrosion of the metal surface. For all cases, because the failures are not cohesive in the adhesive, bond performance might be further improved using even better inhibitors.

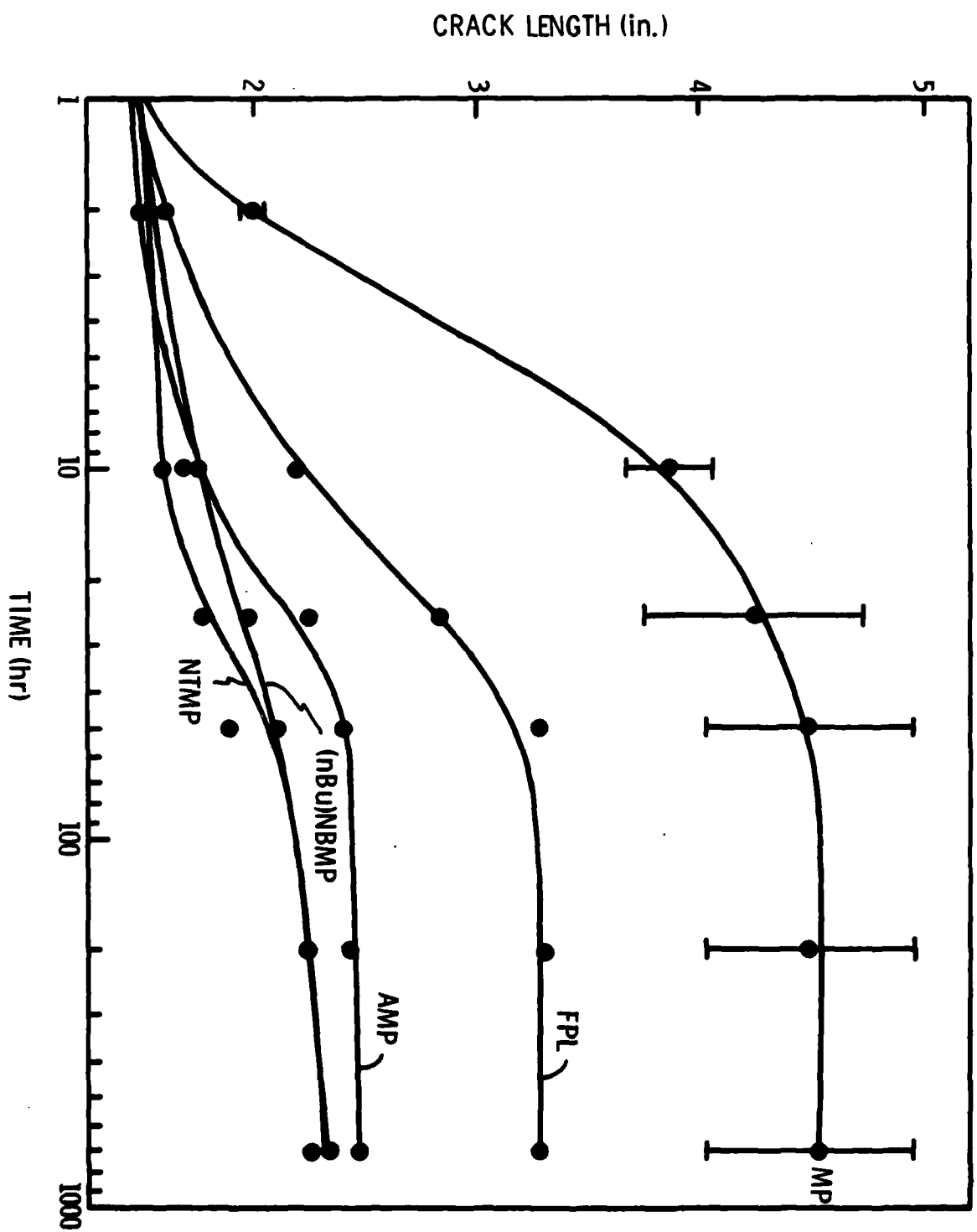


Figure 3. Wedge-test results (crack length as a function of time) for FPL adherends treated in solution of MP, AMP, (*n*Bu)<sub>2</sub>NBMP, and NTMP and for untreated FPL adherends.<sup>(11)</sup>

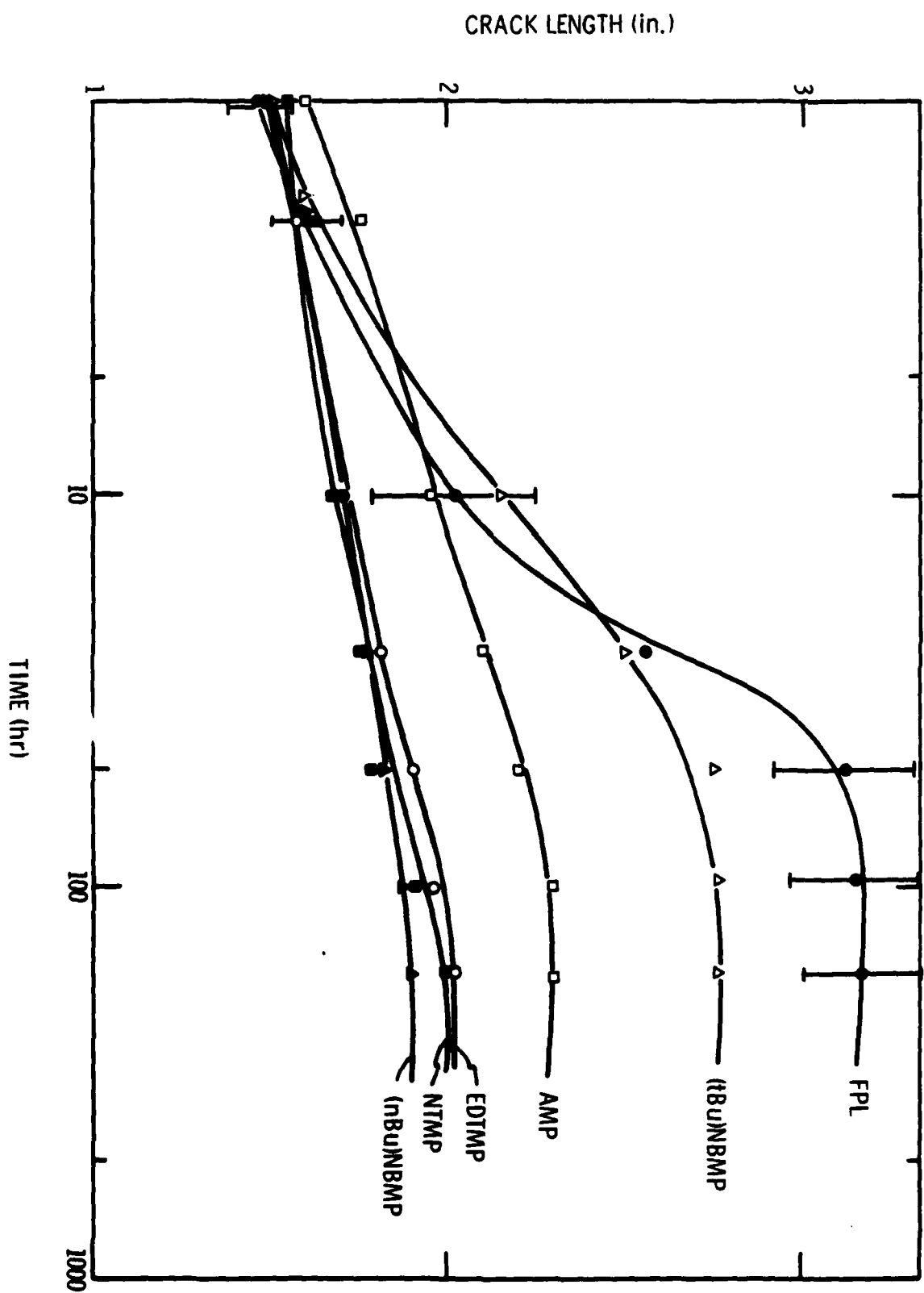


Figure 4. Wedge-test results (crack length as a function of time) for FPL adherends treated in solutions of AMP, (nBu)NBMP, NTMP, and EDTMP.

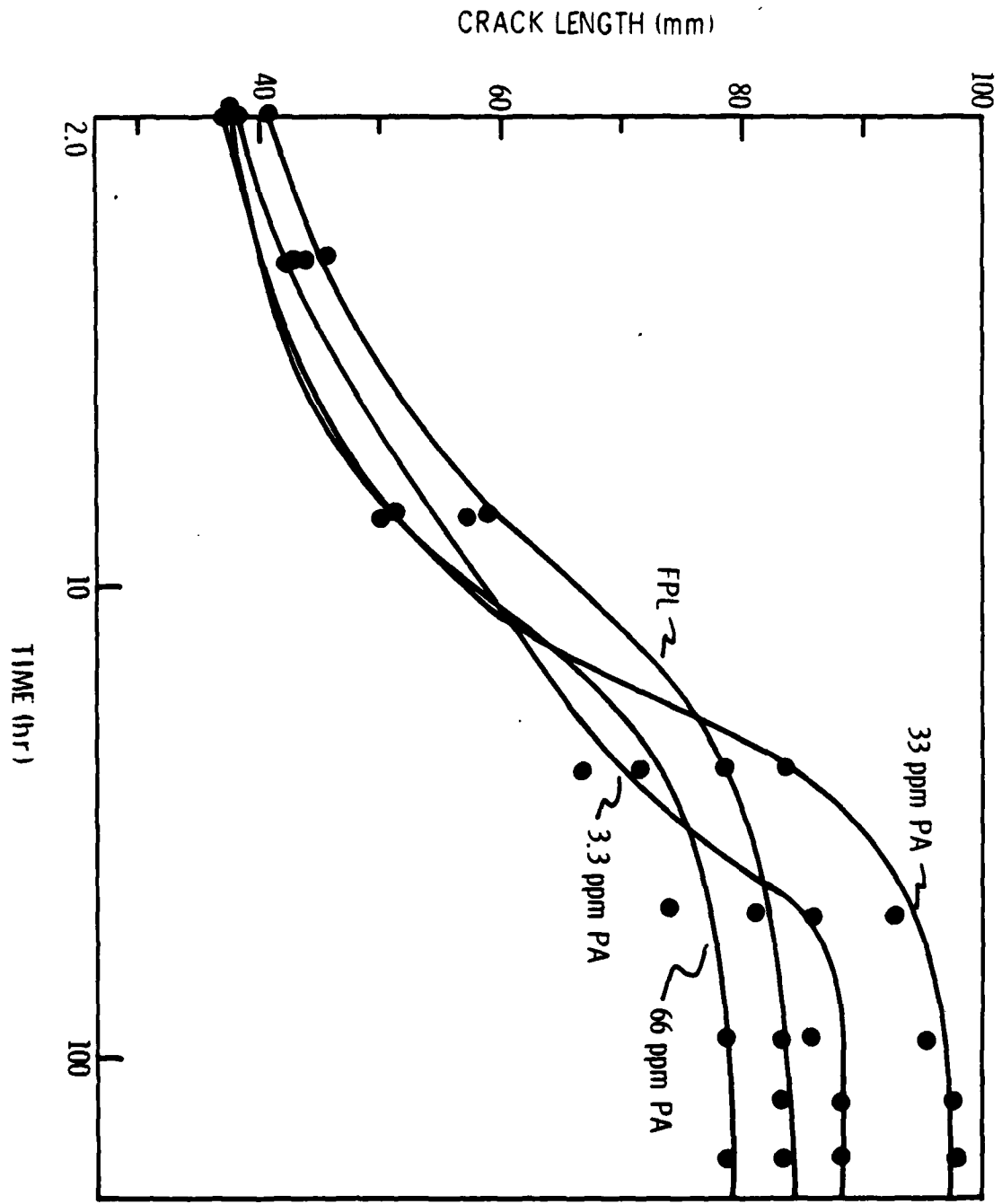


Figure 5. Wedge-test results (crack length as a function of time) for FPL adherends treated in solutions of PA.<sup>(9)</sup>

Table V

Surface Composition of Wedge Test Surfaces (at. %)

Group	Inhibitor	Al		O		C	
		M <sup>a</sup>	A <sup>b</sup>	M	A	M	A
	Adhesive	--	0	--	8	--	92
	Control	22	24	44	47	34	30
I	MP	20	0	50	21	29	78
I	PA (66 ppm)	25	2	49	25	25	73
II	(t Bu)NBMP	30	29	59	58	10	12
III	NTMP	30	14	56	38	13	47
III	EDTMP	29	19	59	45	12	36
III	(n BU) NBMP	31	30	56	58	13	11

a metal side

b adhesive side

The micrographs of the near-crack-tip region of NTMP-treated panels reveal a "shiny" aluminum area right at the crack tip and a "dull" region further along the crack (Fig. 6). Upon closer examination, the shiny area exhibits an FPL morphology whereas the dull area exhibits the cornflake morphology of a hydrated surface.<sup>(3)</sup> In this case, the crack has apparently propagated in advance of the hydration of the aluminum oxide; only after additional exposure to the moist environment does hydration occur.

In other specimens that show improvement over the control, bond failure apparently occurred as a result of hydration (Fig. 7). Here we see the crack-tip region of panels treated with AMP and (nBu)NBMP where the cornflake morphology extends up to the crack-tip. More extensive hydration is also seen in some areas, i.e., bayerite crystallites on top of the boehmite.

Using these results and what is mentioned in the discussion presented in Section IV, we subsequently designed, synthesized, and tested the three inhibitors shown in Fig. 2: (nBu)ANBMP is an analog of (nBu)NBMP that can chemically react with an epoxy adhesive and 2 $\phi$  and 2pA are an inert/reactive pair similar to EDTMP. In wedge tests using these and some of the earlier compounds, (Fig. 8), treatment with four of the inhibitors lead to improved performance over that of NTMP-treated structures, but equivalent to that of the NTMP-treated structures of Fig. 4. In no case was the performance as good as the adhesive-limited results. Macroscopically, failure occurred interfacially. We are currently using XPS and XSEM to determine the exact locus of crack propagation and will discuss our findings in a latter report.

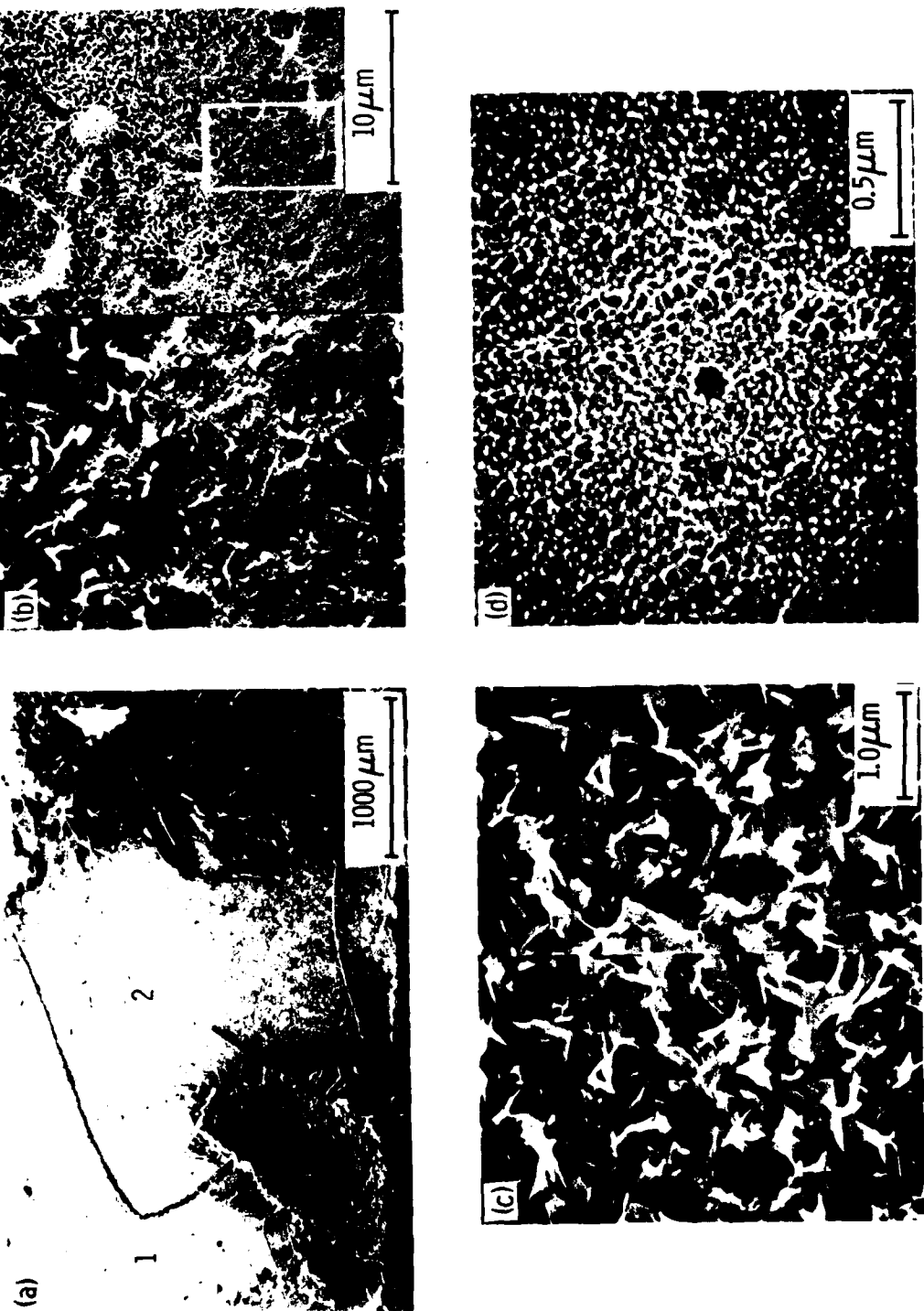


**Figure 6.** Scanning electron micrographs of the near-crack-tip region of the aluminum side of an NTMP-treated FPL-etched wedge test specimen: a) low magnification view showing 1) the dull aluminum area and 2) the shiny aluminum area, and the cohesive failure in the adhesive after the wedge test was completed (at right); b) the beginning of hydration in the boundary region between dull and shiny areas, enlargement of the blocked-in area in inset is at left; c) higher magnification stereo view of the dull area showing the corn-flake boehmite structure; and d) high-magnification stereo view of the shiny area showing the original FPL morphology.

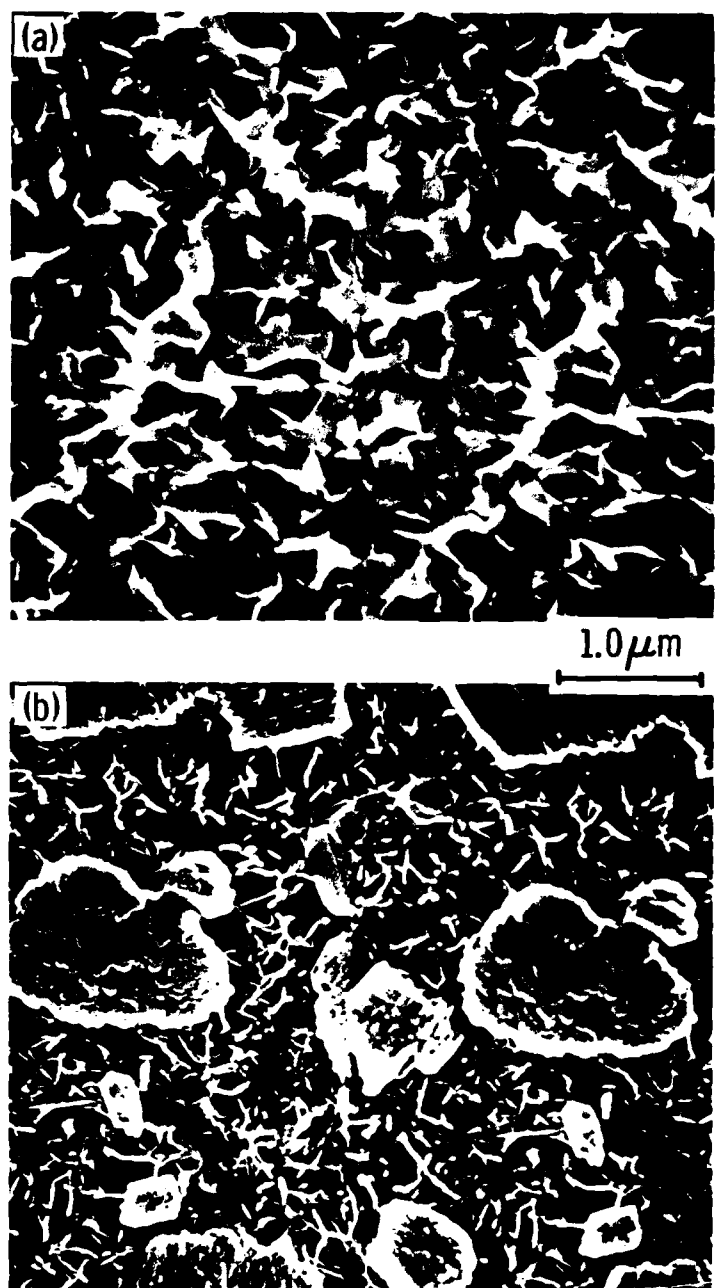


**Figure 7.** Scanning electron micrographs of the near-crack-tip region of the aluminum side of two inhibitor-treated FPL-etched wedge test specimens: a) AMP-treated surface exhibiting cornflake (boehmite) morphology and b) (nBu)NBMP-treated surfaces exhibiting bayerite crystallites on top of boehmite.

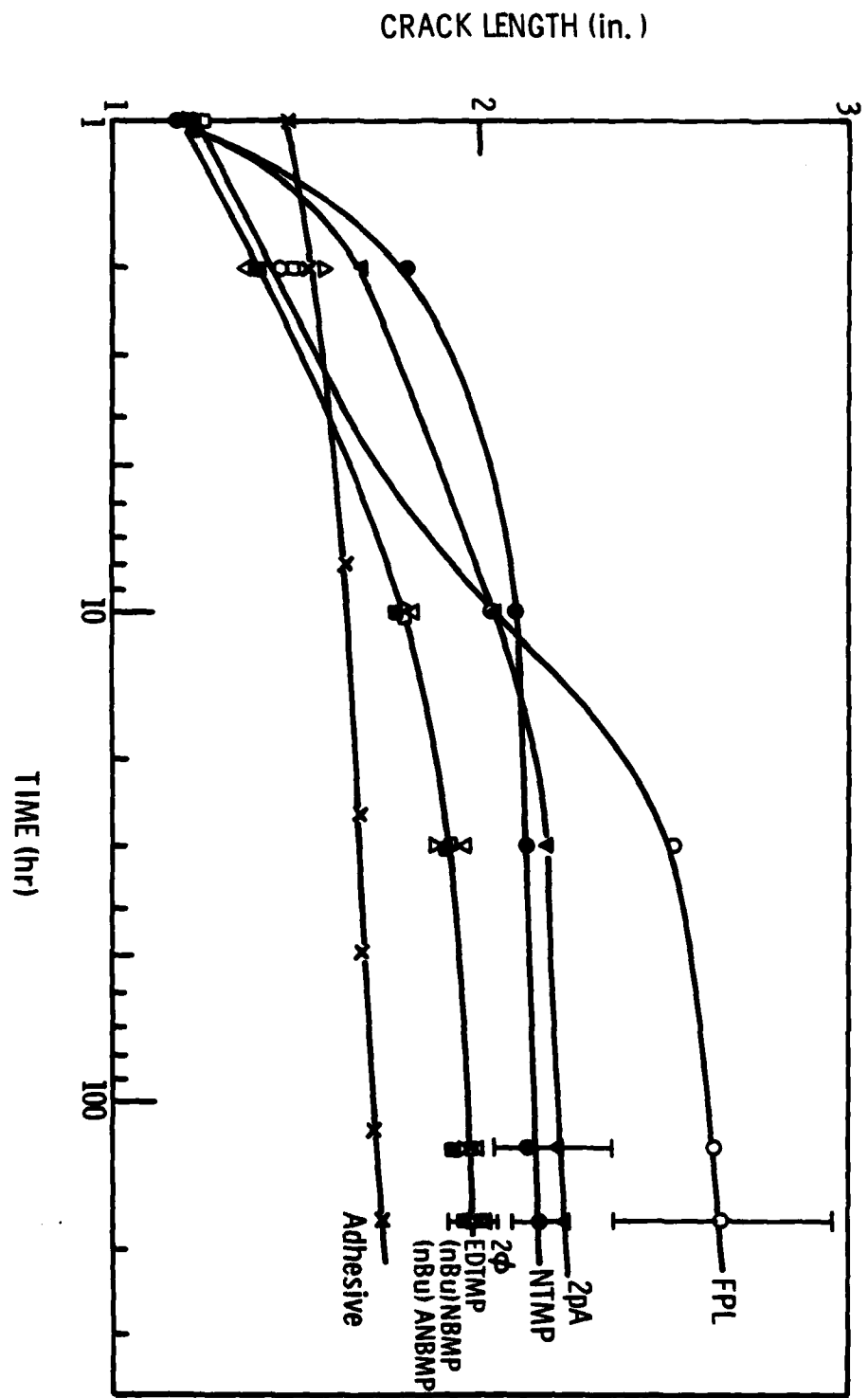


Figure 8. Wedge-test results (crack length as a function of time) for FPL adherends treated in solutions of  $2\Phi$ , NTMP,  $2\Phi$ , EDTMP, (*n*Bu)NBMP, and (*n*Bu)ANBMP and for untreated FPL adherends.

#### IV. DISCUSSION

##### A. INITIAL DRY STRENGTH

Use of epoxy adhesives in T-peel and double-lap-shear tests of treated and untreated structures demonstrates that optimum initial dry strength is exhibited by the control specimens since failure was cohesive in the adhesive. Consequently, no improvement was expected or observed for inhibitor-treated adherends. The observation that the treated specimens exhibit dry performance equal to that of the controls indicates that the interfacial strength between the oxide and adhesive remains stronger than the cohesive strength of the adhesive.

The small degradation of T-peel strengths of primed, treated structures bonded with the nitrile phenolic adhesive suggests that these inhibitors may not be compatible with all types of adhesives. In these cases, failure occurred within the polymer system, possibly at the primer-adhesive interface. The inhibitors, then, do not weaken the primer-aluminum oxide interface below the cohesive strength of the polymer system, but may inhibit curing in the polymer, thereby weakening the bond. Clearly the compatibility of an inhibitor with a non-epoxy-based adhesive system must be determined before use.

##### B. BOND DURABILITY

The wedge test results allow us to identify two properties of an ideal inhibitor: compatibility with the adhesive/primer, and coupling to the adhesive which was first proposed in a previous report,(11). As the T-peel results show, compatibility can be important, and, as the wedge tests for MP and PA indicate, this requirement becomes much more stringent during exposure to a humid environment. Under such conditions, MP treatment accelerates bond

failure compared to FPL adherends whereas PA treatment does not change performance although it does confer hydration-resistance to the unbonded surface.<sup>(10)</sup> For both bonds, the crack propagated along the adhesive-oxide interface which the inhibitors apparently weakened and made susceptible to moisture attack by passivating the adherend surface or preventing the formation of adhesive-oxide or adhesive-inhibitor chemical bonds. In either case, compatibility of the inhibitor with the adhesive in both dry and wet environments is necessary to prevent rapid bond failure.

The other criterion for a good inhibitor - coupling to the adhesive - can be deduced from the micrographs of the crack-tip region and from the relative performance of adherends treated with the two (Bu)NBMP compounds. Samples treated with (tBu)NBMP and AMP exhibit only moderate bond durability. Failure occurs as the oxide hydrates, leading to crack propagation within the hydroxide or along the weak hydroxide-metal interface, allowing subsequent hydration of the exposed metal surface.

Even treatment with (nBu)NBMP, although it gives good bond durability, leads to failure by hydration. We attribute the improved performance of these samples over those treated with (tBu)NBMP to a molecular mechanical interlocking or good dispersion of the n-butyl tail in the polymeric adhesive. This mechanical coupling would make the inhibitor less vulnerable to aqueous attack and improve bond durability, but may be insufficient to fully compensate for the reduced number of inhibitor-oxide bonds (relative to NTMP). As a result, (nBu)NBMP treatment fails to provide consistently superior performance to NTMP treatments. A similar effect may occur with AMP treatments where the addition of the amino group to MP dramatically changes the performance of the respective bonds. This amino group is capable of reacting with the epoxy adhesive, thus strengthening the inhibitor-adhesive interface. At the same time, by making a less soluble complex, the inhibitor probably increases the hydration resistance of the oxide, even though the residual adsorbed water that remains on the surface following AMP adsorption<sup>(11)</sup> can act as initiation sites for hydration. These initiation

sites prevent the hydration resistance from becoming as high as that of NTMP-treated oxides.

The failure of the NTMP-treated specimens, on the other hand, occurs not upon hydration, but prior to it. In these cases, the hydration rate is slowed sufficiently so that it is no longer the limiting factor in bond durability. Instead, failure occurs along the inhibitor-adhesive interface, and only after subsequent exposure does the oxide surface hydrate. These results suggested that further improvement in bond durability could be achieved by strengthening the inhibitor-adhesive interface either by chemical or mechanical coupling while maintaining strong inhibitor-oxide bonding and was the rationale behind the second generation of inhibitors (Fig. 2).

Initial wedge test results using the new inhibitors are promising, but somewhat surprising. Based on the arguments just discussed, we would expect 2pA to perform better than 2φ since 2pA was designed as a variant that would react with the epoxy adhesive. Similar considerations exist for (nBu)ANBMP and (nBu)NBMP, although (nBu)NBMP can physically interact with the adhesive by dispersion of the hydrocarbon chain. Further wedge tests are planned to confirm these results and to determine the effect of impurities in the inhibitor solution on the bond performance.

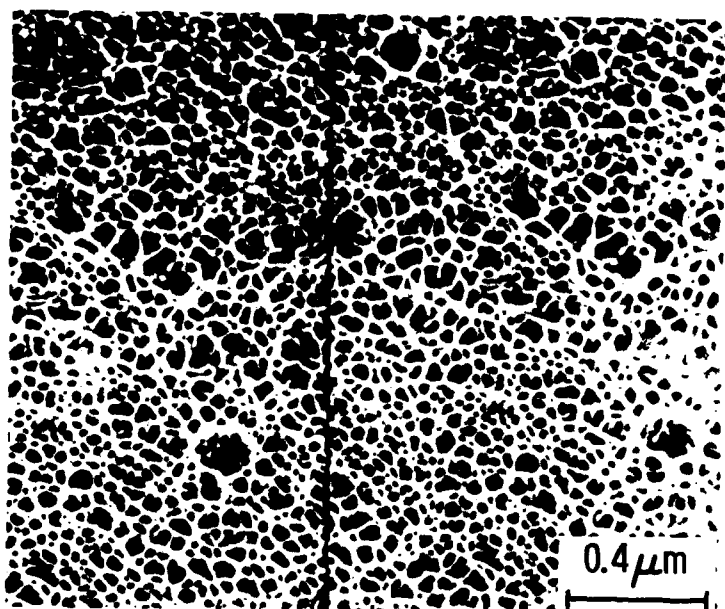
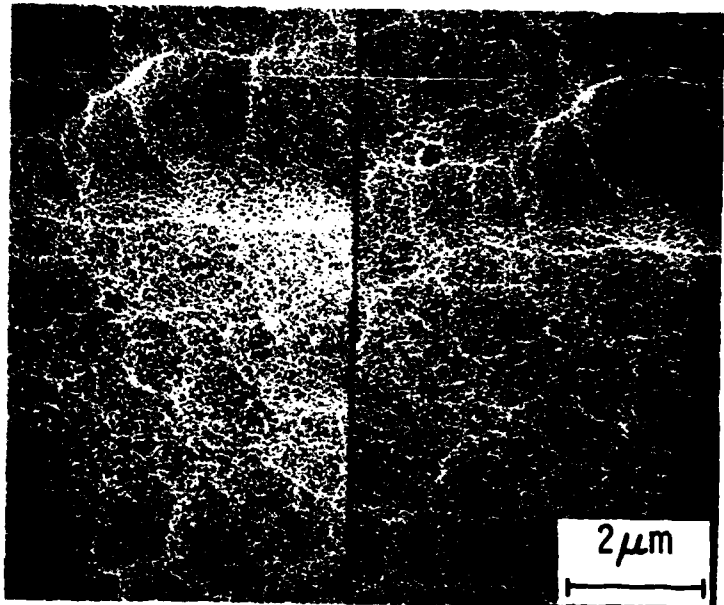
## V. SUMMARY

We have investigated the use of organic hydration inhibitors to improve the durability of adhesively bonded aluminum structures in a hot, humid environment. Several new inhibitors were synthesized and tested using T-peel, double-lap-shear, or wedge tests. Each of the representative inhibitors tested for their effect on initial bond strength was found compatible with several epoxy adhesives in a dry environment. Compatibility with the adhesives in a humid environment, on the other hand, was found to be a more stringent requirement. Examination of the near-crack-tip-region of wedge test specimens treated with NTMP, one of the best inhibitors, revealed that hydration was sufficiently slowed so that crack propagation occurred in advance of hydration. This finding suggested that the final criterion for hydration inhibitors used to promote bond durability (in addition to ones identified previously) is coupling to the adhesive. Compounds designed to meet all the criterion discussed have been synthesized and are currently being tested.

## VI. REFERENCES

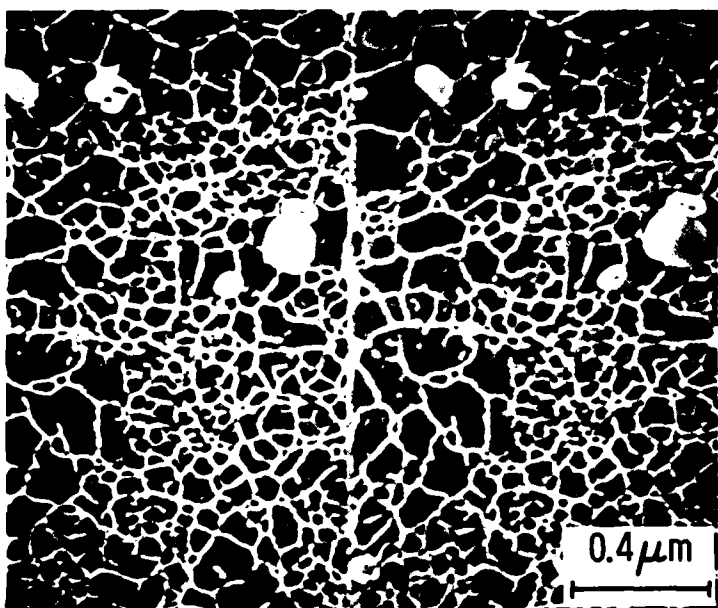
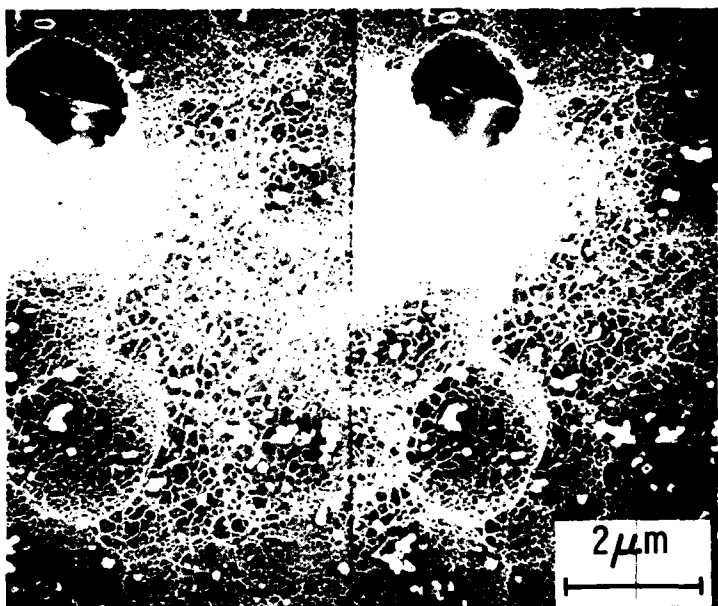
1. H.W. Eichner and W.E. Schowalter, Forest Products Laboratory Report No. 1813, Madison, WI, 1950.
2. G.S. Kabaysaki and D.J. Donnelly, Boeing Corporation Report No. D6-41517, Seattle, WA, February 1974.
3. J.D. Venables, D.K. McNamara, J.M. Chen, and T.S. Sun, *Appl. Surf. Sci.* 3, 88 (1979).
4. D.E. Packham, in Adhesion Aspects of Polymeric Coatings, ed., K.L. Mittal, Plenum, New York, 1983, and the references therein.
5. J.D. Venables, D.K. McNamara, J.M. Chen, B.M. Ditchek, T.I. Morgenthaler, and T.S. Sun, in Proc. 12th Natl. SAMPE Techn. Conf., Seattle, WA, 1980, p. 909.
6. D.A. Hardwick, J.S. Ahearn, and J.D. Venables, MML TR 82-23c, End-of-Second-Year Report under ONR Contract N00014-80-C-0718, Martin Marietta Laboratories, Baltimore, MD.
7. D.A. Hardwick, J.S. Ahearn, and J.D. Venables, *J. Mater. Sci.* 19, 223 (1984).
8. G.D. Davis, J.S. Ahearn, L.J. Matienzo and J.D. Venables, accepted by *J. Mater. Sci.*
9. J.S. Ahearn, G.D. Davis, T.S. Sun, and J.D. Venables in Adhesion Aspects of Polymeric Coatings, ed., K.L. Mittal, Plenum, New York, 1983.
10. J.S. Ahearn, G.D. Davis, A.I. Desai, and J.D. Venables, MML TR 81-46c, End-of-First-Year Report under ONR Contract N00014-80-C-0718, Martin Marietta Laboratories, Baltimore, MD.
11. G.D. Davis, J.S. Ahearn, and J.D. Venables, MML TR 83-34c, End-of-Third-Year Report under ONR Contract N00014-80-C-0718, Martin Marietta Laboratories, Baltimore, MD.
12. G.D. Davis, T.S. Sun, J.S. Ahearn, and J.D. Venables, *J. Mater. Sci.* 17, 1807 (1982).

2024 FPL



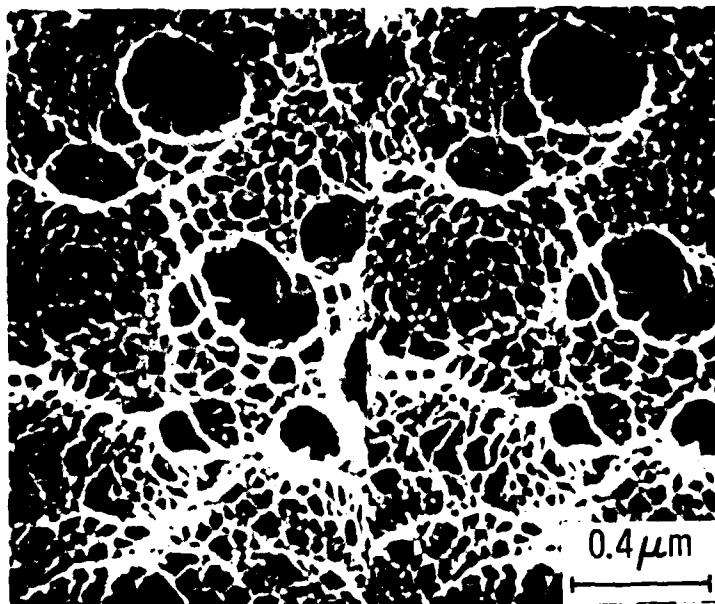
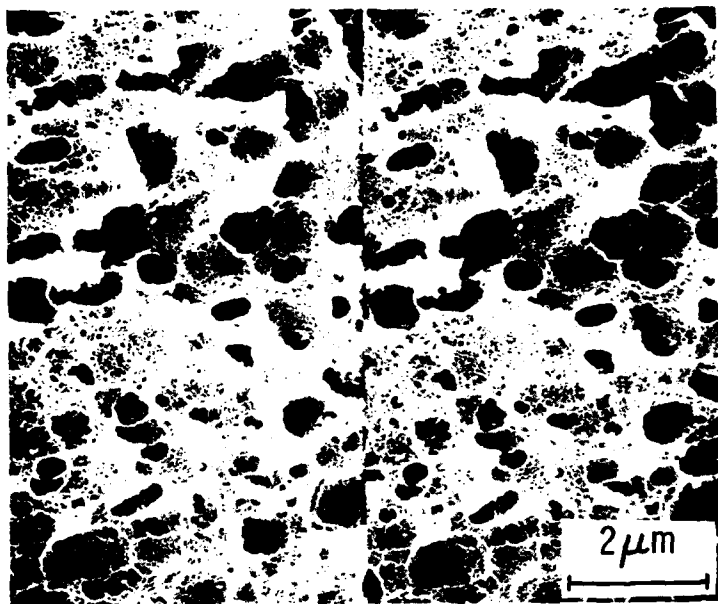
A1. XSEM micrographs of the FPL-etched 2024 Al surface.

6061 FPL



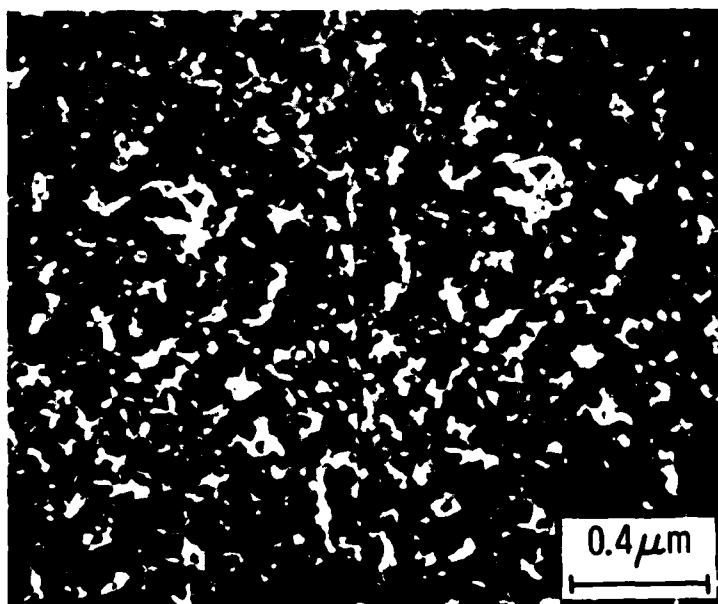
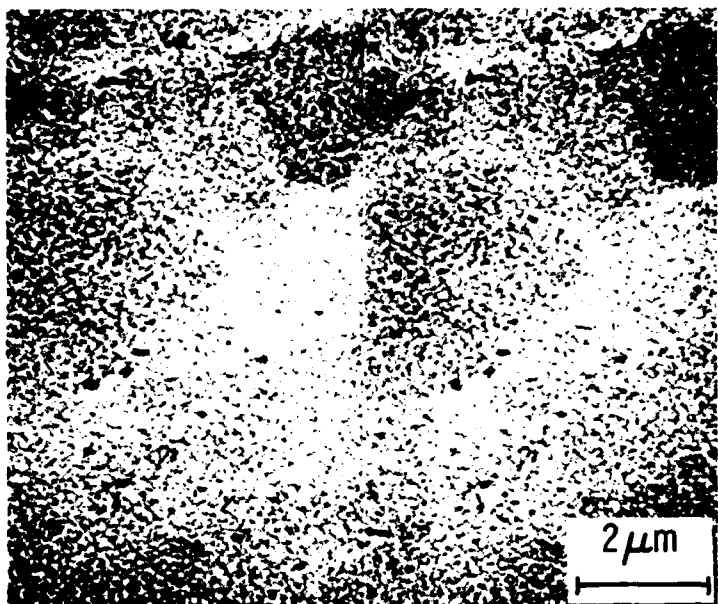
A2. XSEM micrographs of the FPL-etched 6061 Al surface.

7005 FPL



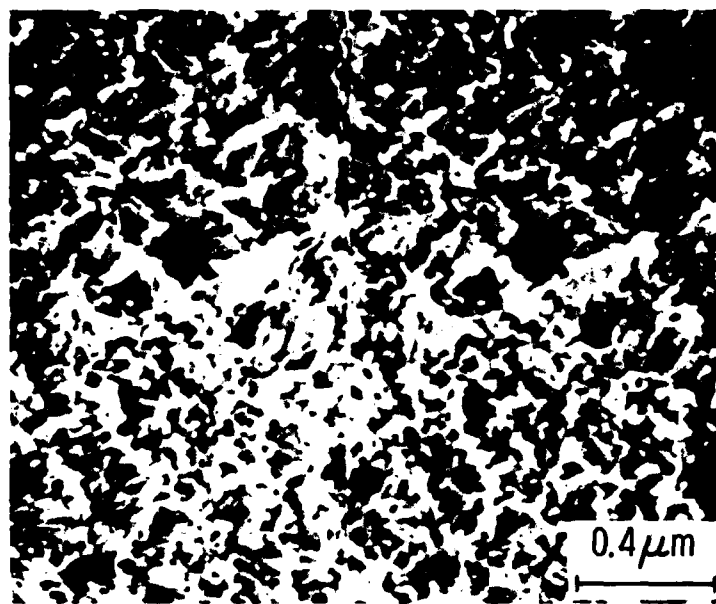
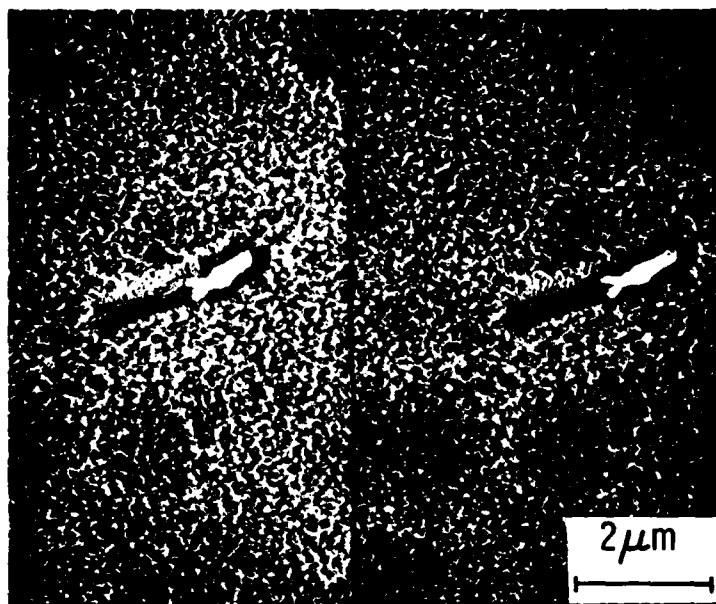
A3. XSEM micrographs of the FPL-etched 7005 Al surface.

2024 PAA



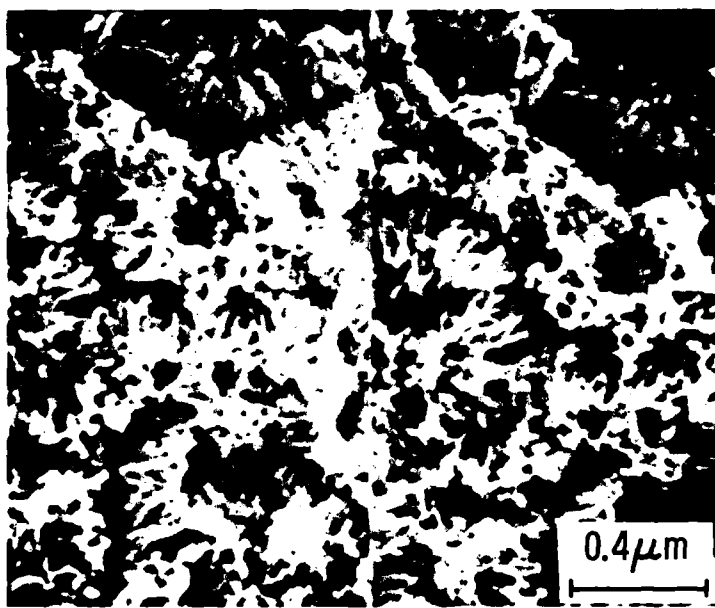
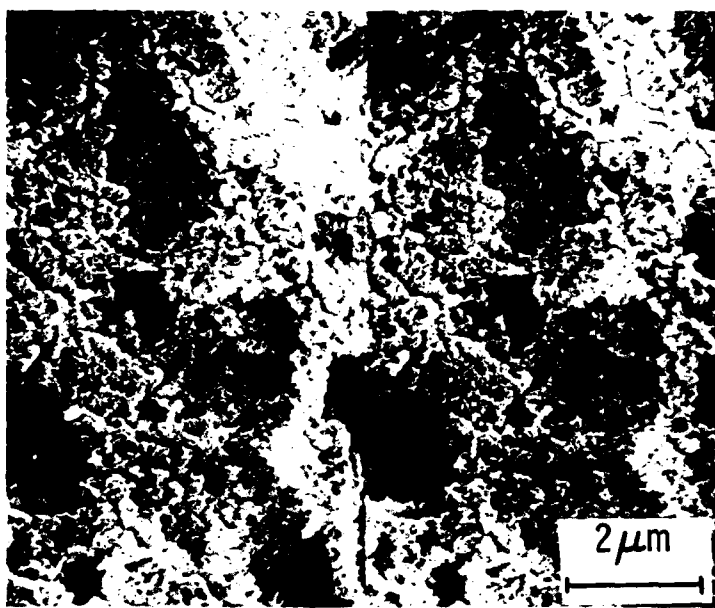
A4. XSEM micrographs of the PAA-treated 2024 Al surface.

6061 PAA



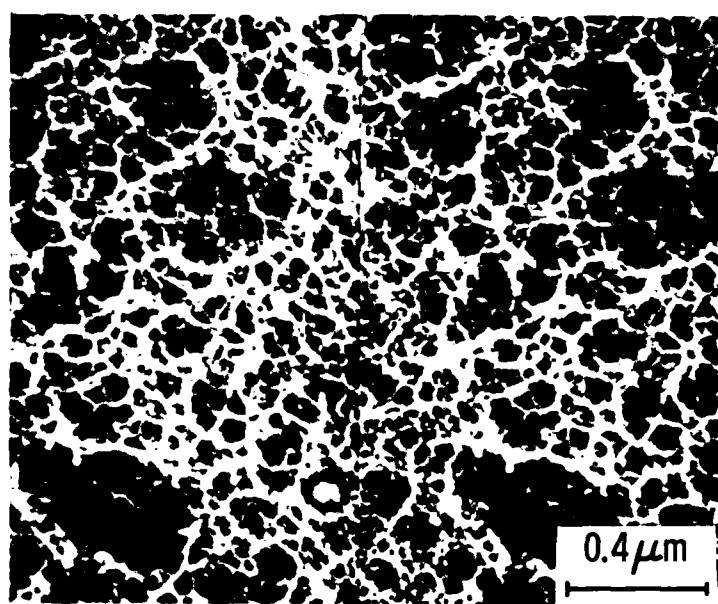
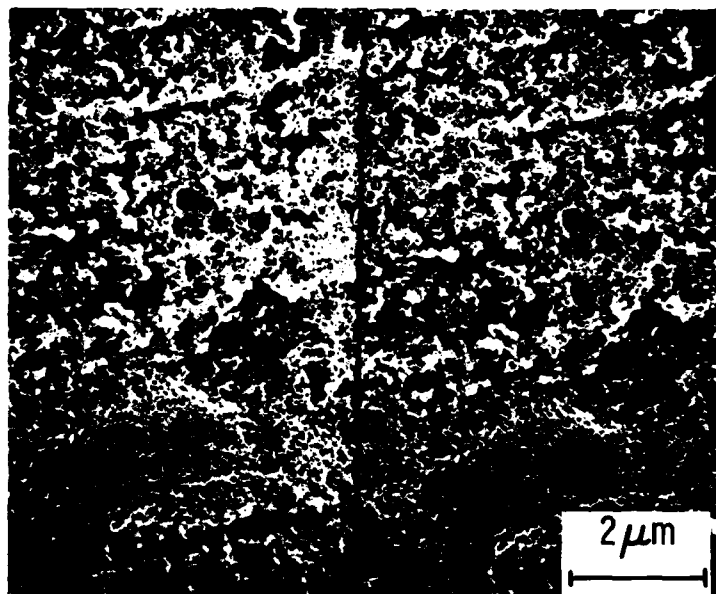
A5. XSEM micrographs of the PAA-treated 6061 Al surface.

7005 PAA



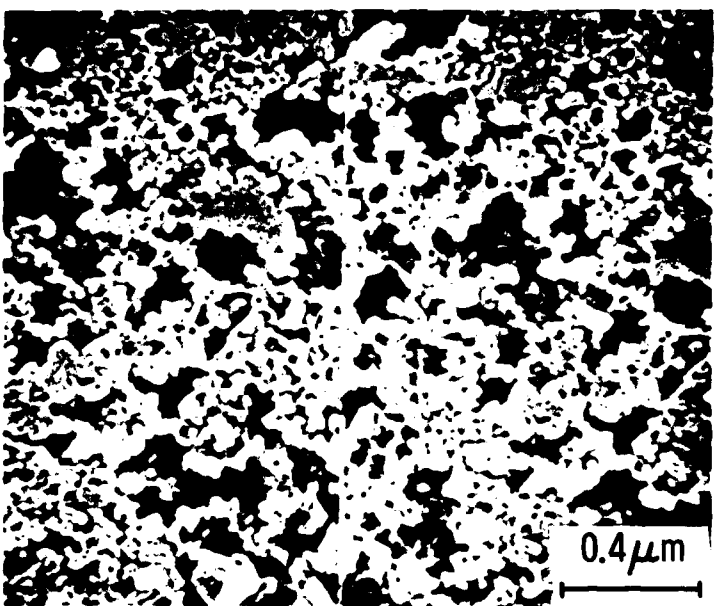
A6. XSEM micrographs of the PAA-treated 7005 Al surface.

2024 P2



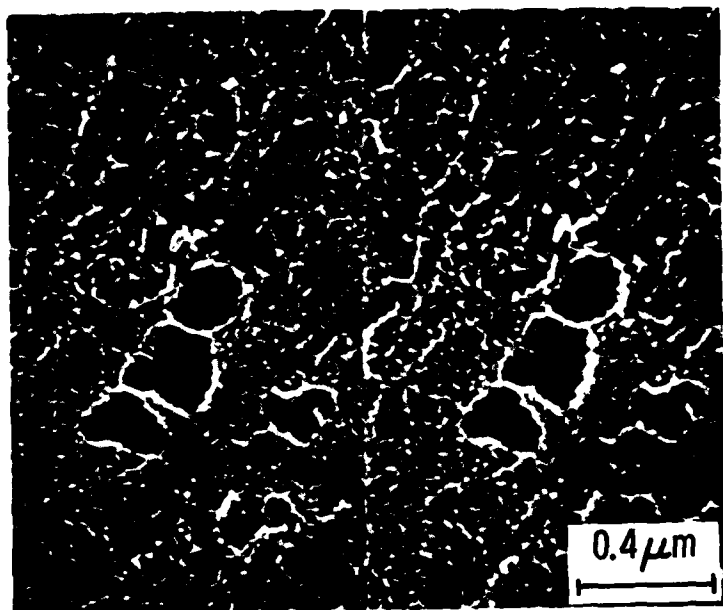
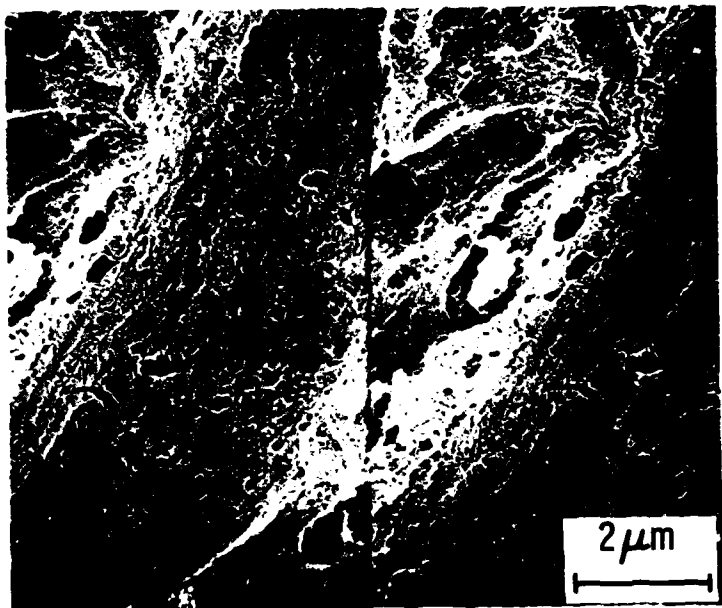
A7. XSEM micrographs of the P2-etched 2024 Al surface.

6061 P2



A8. XSEM micrographs of the P2-etched 6061 Al surface.

7005 P2



A9. XSEM micrographs of the P2-etched 7005 Al surface.

## APPENDIX A: OXIDE MORPHOLOGIES

The oxide morphologies of 7005 and 6061 Al alloys have been compared to those of 2024 Al for three surface pretreatments used or potentially used for adhesive bonding: FPL,(A1) PAA,(A2) and P2.(A3) The FPL etch is widely used in the aerospace industry and has served as our standard preparation during this contract. The PAA treatment, which is becoming more commonly used, also has been used during some aspects of this investigation. In contrast, the P2 process, a ferric sulfate/sulfuric acid etch which was developed as a chromate-free alternative to the FPL etch, has not yet achieved wide use.

The treatment procedures for each of these processes are given in Table AI; the solutions required are given in Table AII for each treatment.

As shown in Figs. A1-A3, each alloy upon etching in an FPL solution develops similar microrough surfaces which are necessary for good adhesive bond strength i.e., low cell walls with protruding whiskers. However, differences in the cell dimensions are observed. The most open structure is seen in 6061, which has an average pore diameter of ~ 1000 Å, followed by 7005 and 2024 with pore cells of ~ 600 Å and ~ 400 Å, respectively. The lower magnification micrographs shows that the 7005 surface is more pitted than the other alloys.

Less variation is observed is the microroughness of the phosphoric-acid-anodized-surfaces (PAA) (Figs. A4-A6). Each oxide is in the form of small (~ 400 Å), well developed cells with projecting whiskers that should be capable of mechanically interlocking with an adhesive or primer. Again at lower magnification the 7005 surface is rougher with some pitting and agglomeration of cells.

Finally, the greatest alloy to alloy variation is seen in the morphologies of the three P2-etched surfaces. (Figs. A7-A9). The structure of the 2024 oxide appears to be intermediate between its corresponding FPL and PAA oxides and resembles a similar oxide on 2219 Al, which has been shown to

have excellent adhesive bond capabilities.<sup>(A4)</sup> The 6061 surface, on the other hand, is a more dense oxide that might not allow adequate penetration of the adhesive. The 7005 oxide is less developed with a very fine microroughness.

In summary, both the FPL and PAA processes develop morphologies suitable for adhesive bonding on all three alloys investigated. The P2 process results in an appropriate oxide for 2024 Al, but the suitability of the oxides it produces on 6061 and 7005 Al needs to be determined with mechanical testing.

TABLE AI

ALUMINUM PRETREATMENTS FOR ADHESIVE BONDING

Forest Products Laboratory

1. Immerse panel in a TURCO solution at 150°F and agitate for 15 minutes.  
Rinse with deionized, distilled water.
2. Immerse in FPL solution at 150°F and agitate for 15 minutes.  
Rinse with deionized, distilled water.  
Dry with room temperature forced air.

Phosphoric Acid Anodization

1. Perform steps 1 and 2 of FPL process.
2. Anodize in phosphoric acid solution at room temperature for 20 minutes at 10Vdc. Leave in tank for 2 minutes after power shut off.  
Rinse with deionized, distilled water.  
Dry with room temperature forced air.

P2

1. Perform step 1 of FPL process.
2. Immerse in P2 solution at room temperature\* with agitation for 15 minutes.  
Rinse with deionized, distilled water.  
Dry with room temperature forced air.

---

\* Specifications originally suggested 63°C. Mechanical tests at the Laboratories have shown equivalent performance of panels treated at 63°C and room temperature.

TABLE AII  
PRETREATMENT SOLUTIONS

TURCO Degreaser (alkaline cleaner)

160 g TURCO 4215  
10 ml TURCO additive  
Add deionized, distilled water to make 4 liters

Optimized FPL

241 g  $\text{Na}_2\text{Cr}_2\text{O}_7 \cdot 2\text{H}_2\text{O}$   
692 ml 96%  $\text{H}_2\text{SO}_4$   
7.5 g 2024 Al (seeding)  
Add deionized, distilled water to make 4 liters  
Heat mixture to  $80^\circ\text{C} \pm 10^\circ\text{C}$  to dissolve seeding material

Phosphoric Acid

10 wt% 85%  $\text{H}_3\text{PO}_4$

P2

370g 96%  $\text{H}_2\text{SO}_4$   
150g  $\text{Fe}_2(\text{SO}_4)_3 \cdot x\text{H}_2\text{O}$   
Add to 1l deionized, distilled water

REFERENCES

- A1. H.W. Eichner and W.E. Schowalter, Forest Products Laboratory Report No. 1813, Madison, WI 1950.
- A2. G.S. Kabayaski and D.J. Donnelly, Boeing Corporation Report No. D6-41517, Seattle, WA, February 1974.
- A3. N.L. Rogers, Proc. 13th Natl. SAMPE Techn. Conf., Mt. Pocono, PA, 1981, p. 640.
- A4. J.S. Ahearn and A.I. Desai (unpublished results).

## APPENDIX B: SYNTHESIS

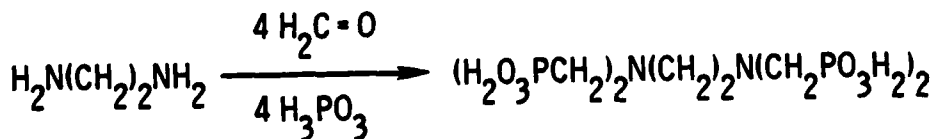
### PHOSPHONATION (General)

The preparation of  $\alpha$ -aminomethylphosphonic acids involves a Mannich-type reaction based on the method of Moedritzer and Irani.(B1) In an appropriate-sized round-bottomed flask, x moles of the amine were dissolved in approximately 5 times the volume of distilled water. Concentrated hydrochloric acid was added slowly in a molar quantity equivalent to the total number of amino groups in the reactant molecule. Phosphorous acid ( $H_3PO_3$ ), in a molar quantity equal to the total number of hydrogens on the amine groups, was dissolved in a minimum volume of water and added to the neutralized diamine. Formaldehyde (37%, in a quantity 2.5 times the molar equivalent of added  $H_3PO_3$ ) was then added to the contents with stirring for at least 30 minutes. The flask was then heated to 80°C and the solution stirred for 60 minutes at this temperature.

The cooled liquid solution was evaporated under vacuum and the resulting viscous residue washed with acetone or ethanol to yield a hygroscopic solid product. The filtered crystals were washed with anhydrous ether (or acetone) and stored in a dessicator, under vacuum.

### PREPARATION OF ETHYLENEDIAMINE TETRAMETHYLENE PHOSPHONIC ACID (EDTMP)

#### REACTION



## EXPERIMENTAL (Phosphonation)

Ethylenediamine (17 ml, 0.25 mol) was dissolved in 100 ml of water in a 3-necked 500 ml round-bottomed flask. To this solution was slowly added 82 ml (1.0 mol) of concentrated hydrochloric acid to neutralize the amine. A concentrated aqueous solution of phosphorous acid (82g, 1.0 mol) was poured into the flask with stirring. The solution was brought to reflux temperature and 160 ml (2.14 mol) of 37% formaldehyde added dropwise over the course of 1 hr. The flask was then heated overnight (18 hr) at 70°C.

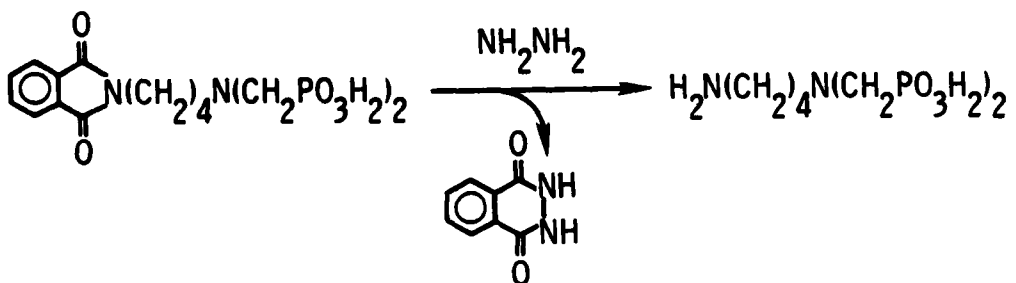
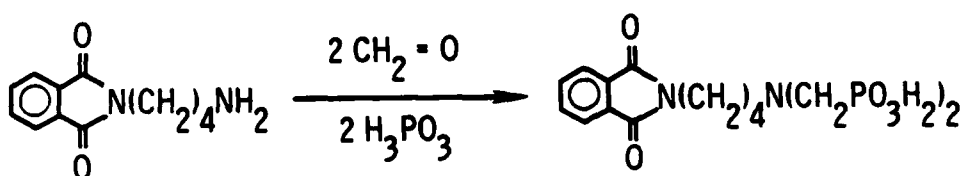
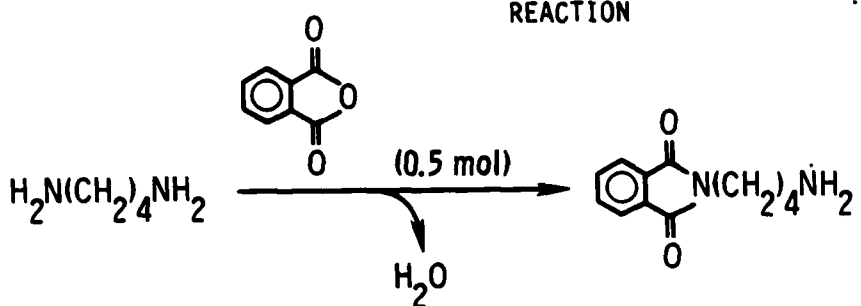
The reaction was terminated only when the  $^{31}\text{P}$  NMR spectrum of the contents indicated no further increase in the phosphonate peak amplitude. The orange product was allowed to cool to room temperature and a solid product precipitated out of the solution. The crystals were washed with acetone: water (5:1, v:v) and ethyl ether, dried and stored under vacuum.

Analytical	<u>C</u>	<u>H</u>	<u>N</u>	<u>P</u>
Calc.	16.51	4.59	6.42	28.44
Found	16.73	4.80	6.40	28.80

mp 185-190°C

PREPARATION OF n-BUTYLAMINO-NITRILOBISMETHYLENE PHOSPHONIC ACID  
[(nBu)ANBMP]

REACTION



EXPERIMENTAL

Reaction 1) Protection of Amine Group. To a solution of 10.0 g (0.114 mol) of 1,4-diaminobutane in 20 ml toluene was added 16.83 g (0.114 mol) of finely ground phthalic anhydride dissolved in toluene, dropwise with stirring. An additional 130 ml of toluene was added to the flask and the

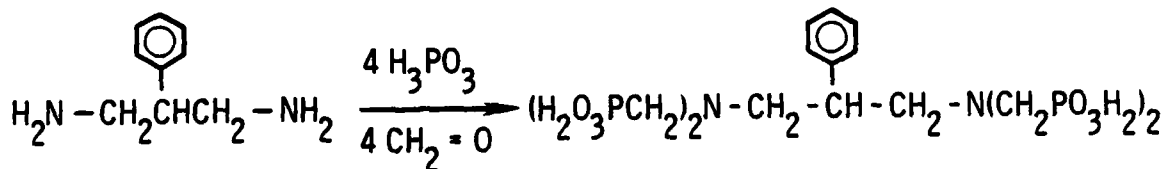
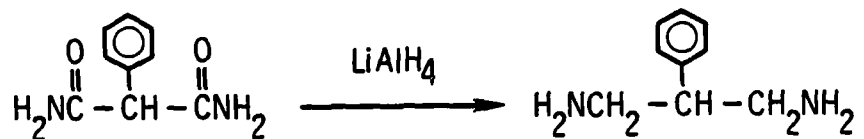
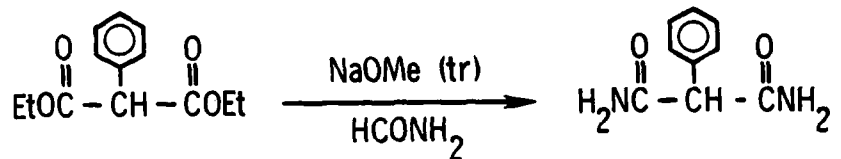
contents brought to reflux. Water was separated using a Dean-Stark apparatus and the remaining solvent removed under vacuum. The solid phthalamide product was filtered, washed with cold water and dried.

Reaction 2) Phosphonation of Free Amine Group. To 6.54 g of the phthalimide suspended in 20 ml of water was added 10 ml of concentrated HCl cautiously, with stirring. A concentrated solution of phosphorous acid (4.92 g, 0.060 mol) was then added and the flask contents brought to reflux temperature. Formaldehyde (12 ml, 0.161 mol) was added dropwise to the mixture, which was heated at reflux temperature for 24 hr. The solid product was filtered, washed with methanol and dried.

Reaction 3) Hydrolysis. A solution of 15.0 g (0.037 mol) of the phosphonate product and 5.4 ml of 1 M hydrazine in 115 ml ethanol was heated under reflux for 2 hr. After removing the solvent by rotary evaporation, 80 ml of water was added and the solution brought to pH 6 with acetic acid. The acidified solution was heated at 65°C for 1 hour. Upon cooling a white solid precipitated out which was filtered and washed with methanol.

PREPARATION OF 2-PHENYL-1,3-DI (NITRILOBISMETHYLENE  
PHOSPHONIC ACID) PROPANE (2 φ)

REACTION



EXPERIMENTAL

Reaction 1) Amidation of diethylphenylmalonate. (B2) To a mixture of 100 g (0.423 mol) of phenyldiethylmalonate and 35.6 ml (0.9 mol) of formamide was added 2.43 g (0.045 mol) of sodium methoxide\* slowly with stirring. The solution was heated at reflux temperature overnight and cooled. Removal of the solvent under vacuum left a residue, which was washed with cold water and ether and dried.

---

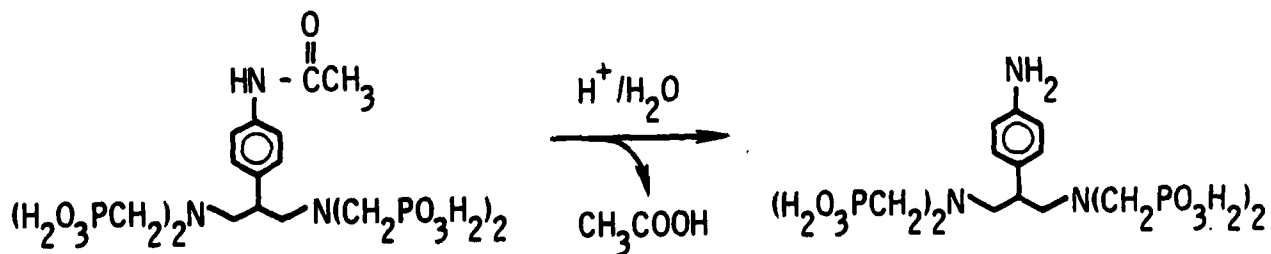
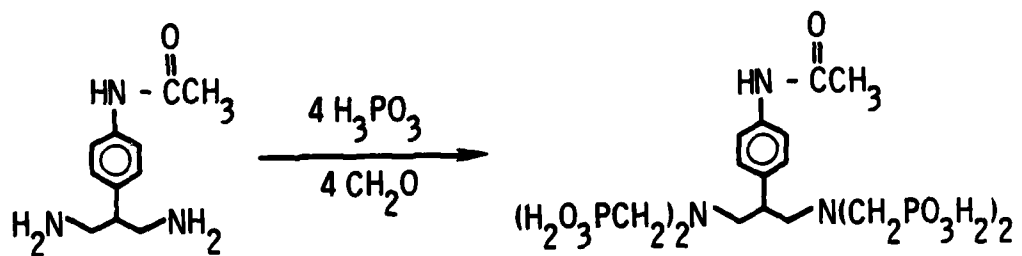
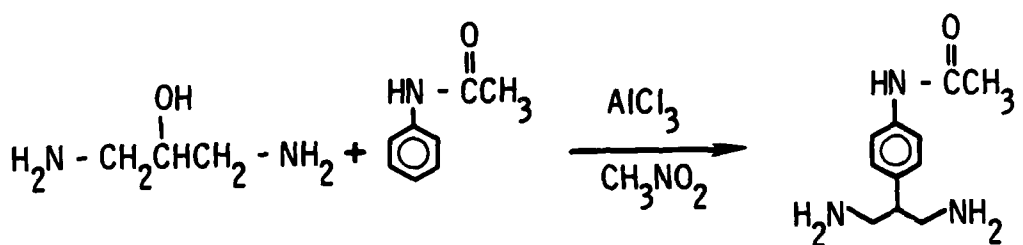
\* Prepared by adding solid sodium (dry) to anhydrous methanol and removing the excess solvent by rotary evaporation.

Reaction 2) Reduction of Diamide. In a 3-necked 1 l round-bottomed flask equipped with a reflux condenser and a dropping funnel was placed a suspension of 3.9 g (0.10 mol) of lithium aluminum hydride in 50 ml of anhydrous ether. While the mixture was being stirred, a solution of 9.7 g (0.04 mol) of 2-phenyl-1,3-propanediamide in 150 ml of anhydrous ether was added at such a rate as to maintain a gentle reflux. The contents were heated under reflux overnight (18 hr). The flask was then placed in an ice bath and fitted with a mechanical stirrer. To the stirred contents were added, in succession, 4 ml of water, 12 ml of a cold aqueous solution of 15% sodium hydroxide, and another 4 ml portion of water. Isolation of the diamine product from copious gelatinous Al salts was accomplished by extraction with dilute acid, followed by re-alkalinization with ammonium hydroxide. This led to minuscule quantities of a viscous product, identified as an amine by its characteristic odor and infrared spectrum.

Reaction 3) Phosphonation of Diamine. The residual amine product (approximately 0.003 mol, 0.5 g) was dissolved in 10 ml of water and subjected to standard phosphonating conditions (0.013 mol  $H_3PO_3$ , 0.028 mol  $CH_2O$ ). The product (0.40 g) was a hygroscopic yellow solid which indicated an amino-phosphonate composition by infrared analysis.

PREPARATION OF 2p-ANILINO-1,3-DI  
(NITRILOBIS METHYLENE PHOSPHONIC ACID) PROPANE (2pA)

REACTION



## EXPERIMENTAL

Reaction 1) Friedel-Crafts Alkylation. To 10 g (0.110 mol) of 1,3-diamino-2-propanol in 50 ml of nitromethane was cautiously added 15 g (0.246 mol) of aluminum chloride powder. After all of the solid had dissolved, 30 g (0.222 mol) of acetanilide was added to the mixture, which was then heated at reflux temperature for 3 hr. After cooling, the solvent was removed by rotary evaporation. The resulting solid product was filtered, washed with methanol and dried.

Reaction 2) Phosphonation. In a 100 ml round-bottomed flask, 5.0g (0.024 mol) of the Friedel-Crafts diamine adduct was dissolved in the minimum volume of distilled water and 10 ml of concentrated HCl added to the flask with stirring. To this mixture was added a concentrated aqueous solution containing 10 g of phosphorous acid. The contents were brought to reflux temperature and 30 ml (0.40 mol) of formaldehyde added dropwise with stirring. The solution was heated overnight, cooled, and rotary-evaporated to furnish a solid product. The crystals were filtered, washed with acetone and dried.

Reaction 3) Hydrolysis. The amine-protected phosphonate product (too hygroscopic for accurate weight determination) was dissolved in 10% nitric acid and heated at 60°C for 2 hr. The cooled contents were subsequently heated with 50% ammonium hydroxide to solubilize the phosphonate salt and the Al salts were filtered out. The solution was re-neutralized and the resulting solid product filtered, washed with cold water and methanol, and dried.

REFERENCES

- B1. K. Moedritzer and R.R. Irani, J. Org. Chem., 31 1603 (1966).  
B2. E.L. Allred and M.D. Hurwitz, J. Org. Chem., 30, 2376 (1965).

**END**

**FILMED**

**12-84**

**DTIC**